Results: A total of 280 responses were submitted from trainees between PGY3 and PGY5. 78% of the responses were concordant with the attending pathologist diagnosis while 22% were discordant (16% same category, 4% higher category, 2% lower category). The interpretations were not likely to change patient management in 91% of the cases.
Conclusions: Our study demonstrates an application of whole slide imaging for improving trainee interpretation of frozen section consultations. Responses from residents and fellows correlated well with actual interpretations from attending pathologists. Based upon enthusiastic positive feedback from the respondents, ten cases per month will be added to the teaching set on a continuous basis, serving as a permanent database of challenging consultation cases for the training program and will continue to provide insight as to the types of cases trainees may struggle with.

603 The SCVP and AECVP Acute Cellular Rejection Tutorial: A Tool for Pathology Education and Providing Diagnostic Uniformity

The Society for Cardiovascular Pathology, The Association for European Cardiovascular Pathology Working Group. Johns Hopkins, Baltimore, MD.
Background: Endomyocardial biopsy remains the standard by which cardiac rejection is determined in heart transplant recipients. A working formulation created by the International Society for Heart and Lung Transplantation (ISHLT) provides a standardized grading scale used by virtually all transplant centers. Although the ISHLT schema describes the histopathologic findings of rejection, it does not elaborate on the practical issues related to biopsy analysis, nor does it explain many of the pertinent non-rejection findings, including potential artifacts. Consequently, additional supplemental instruction is necessary to increase inter-institutional consistency.
Design: The SCVP and AECVP created a web tutorial (www.scvp.net/acr) covering all aspects of acute cellular rejection. The tutorial covers 7 different facets of interpreting the endomyocardial biopsy, containing over 90 images and a self-administered whole slide image quiz. Since its inception, over 1,200 independent visits have been recorded to the tutorial. A survey to evaluate the utility of the tutorial was added in September, 2013 and has elicited 11 responses to date.
Results: All survey takers were pathologists across a diverse range of expertise with transplant endomyocardial biopsies. Of these respondents, >80% read the entire tutorial and over 90% rated it very good or excellent. Seventy-two percent of respondents found the information very useful and 27% felt the tutorial corrected misconceptions regarding transplant endomyocardial biopsies. Over 90% of respondents would recommend the tutorial to a colleague, while less than 10% would recommend the tutorial to a patient.
Conclusions: The acute cellular rejection tutorial is a useful educational tool for pathologists with any level of expertise in reading endomyocardial biopsies. It should serve to improve cross-institution comparisons. A survey of users found the tutorial to be of great value and worthy of recommendation to colleagues.

604 Resident Learning in Gastrointestinal Pathology: Opportunities for Teaching Improvement

T VandenBoom, H Chen, R Gamez, S Pambuccian, S Yong. Loyola University Medical Center, Maywood, IL.
Background: Gastrointestinal (GI) pathology represents one of the largest portions of the diagnostic services provided by practicing pathologists. Therefore, committed teaching of pathology residents is extremely important. Few studies have been performed to assess the learning curve of residents in GI pathology. Our aim was to objectively evaluate the knowledge progression of a resident in GI pathology and identify key areas for improvement.
Design: Forty commonly encountered GI pathology entities were collected from daily pathology practice. They included 10 benign neoplastic conditions, 10 malignant neoplastic conditions, and 20 nonneoplastic conditions. A single representative H&E stained glass slide was chosen for each case. Pathologists at different training levels, including 5 at PGY 4, 3 at PGY 3, 4 at PGY 2, 4 at PGY 1, and 3 at fellow/attending level, participated together in a test examining 40 glass slides with one minute per case. The data was analyzed using the Microsoft Excel Statistics package.
Results: Statistical analysis of the data revealed the learning curve shown in Figure 1.

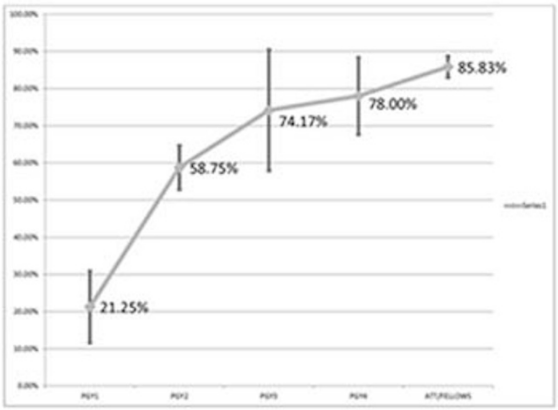

The steepest portion of the learning curve included the PGY 1 and PGY 2 trainees, indicating an accelerated acquisition of knowledge during this time period. The curve begins to plateau from the PGY 3 to fellow/attending levels. Interestingly, PGY 3 and PGY 4 exhibited the largest variation in scores, which we propose may be due to decisions on subspecialization and/or more intense learning in areas of interest for some individuals. Several cases showed overall poor performance (<50% correct) including ganglioneuroma, goblet cell carcinoma, esophageal intramucosal adenocarcinoma, celiac disease, gastric calcinosis, amyloidosis, cryptosporidiosis, and some benign polyps.
Conclusions: GI pathology is a high volume service and it is very important that pathology residents are adequately trained and confident in this subspecialty. Our study shows that we need to capitalize on the early receptive years of pathology resident training. In addition, we need to find ways to interest residents in their latter years in order to continue their growth in GI pathology. Finally, certain areas of poor performance were noted across all levels of training and should be addressed.

605 Curriculum Improvement and Milestone Competence Based on Kolb's Learning Theory

R Zreik, J Stepp, K Walker, C Bloodworth, H Wehbe-Janek, S Dobin, K Jones, A Rao. Scott & White Hospital and Texas A&M HSC, Temple, TX.
Background: Traditional education of pathology residents uses an apprenticeship model with little awareness of student ability or learning styles. The traditional instructor-centric style may fail to engage all learners, possibly impairing their progression through the newly implemented ACGME milestones based competency assessments. This is particularly true in areas such as molecular pathology and informatics. Understanding how learners acquire, retain, and use information may be a key component of resident progression and faculty effectiveness. A well characterized instrument for understanding learning styles is the Kolb's learning style inventory (LSI). We undertook this study to examine if a redesigned genomic curriculum incorporating the core concept areas based on Kolb experiential learning theory and learning styles could be effective for residents and teachers in a pathology residency program.
Design: A total of 15 residents were followed over 18 months. The redesigned genomics curriculum was administered as a 12 hour didactic session (1 hr/week) in molecular pathology and cytogenetics under the direction of 4 faculty, including 2 doctoral level educators. With institutional IRB approval, the Kolb LSI online version was administered prior to the sessions. A pre and post course test, RISE scores, satisfaction surveys and post-course focus group session led by an unbiased third party were utilized to evaluate effectiveness of the course.
Results: The Kolb LSI identified a predominance of converging (n= 7) and assimilating (n=6) styles in the residents. The faculty had diverging and converging styles. The residents' learning styles indicated that the educational activities best suited to them included teaching groups, observation, model making and questions. Relevant resources including articles, lectures, and web based material were made available ahead of the sessions. The sessions were conducted in a case based format accompanied by questions systematically addressing the subject matter with the course directors functioning as experts and coaches. The diverging residents were given a project to facilitate active experimentation. Both ACMGE satisfaction scores and RISE scores showed overall improvement with these methods.
Conclusions: Previous research suggests that learning styles can influence resident performance and progression in the residency program. Understanding and designing educational programs rooted in learning style theory can help the concept of milestone competence.

Endocrine Pathology

606 Two Main Subtypes of Aldosterone-Producing Adrenocortical Adenomas by Morphological and Expression Phenotype

F Al-Hashimi, A Blanes, SJ Diaz-Cano. King's College Hospital, London, United Kingdom; University of Malaga School of Medicine, Malaga, Spain.
Background: Aldosteronism is still a considerable diagnostic challenge generally diagnosed in a 3-tiered system (initial screening, a confirmation of the diagnosis, and a determination of the specific subtype). Since the recognition that ¾ of cases are due to bilateral hyperplasia, the spectrum of adenomas needs further characterization to determine the origin of aldosterone secretion.
Design: We selected unilateral aldosterone-producing adrenocortical adenomas (AP-ACA, 33) responsible of primary aldosteronism defined by WHO criteria from a consecutive series of 98 ACA. We analyzed the histological features (growth pattern, nuclear characteristics, cytoplasmic staining qualities) of the tumor and the expression profile by quantitative RT-PCR of key molecular players of glomerulosa differentiation (SFRP2, β-catenin, AT1R, CYP21 CYP11B2, NURR1 and NUR77) in both the tumor and the surrounding parenchyma. RNA was extracted, cleaned from normal and neoplastic tissues (RNeasy columns), first-strand cDNA synthesized using T7-(dT24)-oligomer and used as template for cRNA synthesis.. The peritumoral parenchyma was also evaluated for the cytohistological features of the glomurulosa and its extension into deep cortex/medulla and periadrenal soft tissues. Quantitative results were cross-validated (expression factor>2, significance<0.01). Variables were studied regarding morphological appearances of the tumor and the status of the peritumoral glomerulosa.
Results: Two main groups of AP-ACA were identified morphologically with a corresponding molecular profile. AP-ACA composed predominantly of clear foamy cells (10) that revealed minimal expression of AT1R, CYP21 and CYP11B2 and AP-ACA composed predominantly of eosinophilic cells (23) expressing significantly high AT1R, CYP21 and CYP11B2. The peritumoral parenchyma revealed functional

hyperplastic glomerulosa in 31 cases, more prominent and with extra-adrenal extension in clear cell AP-ACA.
Conclusions: The common presence of peritumoral hyperplasia suggests a proliferative response of cells to unidentified paracrine/autocrine factor as main mechanism in AP-ACA, which are not involved in glomerulosa differentiation in the clear cell subtype. Clear cell AP-ACA causes a syndrome of aldosteronism characterized by histologic features intermediate between adrenal adenoma and adrenal hyperplasia.

607 High-Density Expression Profiling in Follicular Variant of Papillary Thyroid Carcinomas and Follicular Adenomas of the Thyroid

J Al-Maghrabi, H-J Schulten, R Alotibi, S Karim, K Al-Ghamdi, OA Al-Hamour, E Huwait, M Gari, M Al-Qahtani. Faculty of Medicine. King Abdulaziz University, Jeddah, Saudi Arabia; King Abdulaziz University, Jeddah, Saudi Arabia; Faculty of Medicine, King Abdulaziz University, Jeddah, Saudi Arabia; King Faisal Specialist Hospital and Research Center, Jeddah, Saudi Arabia.
Background: Differential diagnosis of follicular variant of papillary thyroid carcinoma (FVPTC) versus follicular adenoma (FA) remains challenging. RNA expression profiling is an established method to identify diagnostically relevant biomarkers.
Design: Affymetrix HuGene 1.0 ST arrays were used to generate whole transcript expression profiles in 6 FVPTCs, 7 FAs and 9 normal thyroid tissue samples. A p-value with a false discovery rate (FDR) ≤ 0.05 and a fold change > 2 was used as a threshold of significance for differential expression. Spearman's correlation as a similarity matrix was utilized for unsupervised two dimensional hierarchical clustering. Mutational status of BRAF in FVPTCs was established by direct sequencing the hotspot region of exon 15.
Results: We identified nearly 70 transcripts that were significantly differentially expressed between FVPTCs and FAs. Amongst the most significantly upregulated genes in FVPTCs were UDP-N-acetyl-alpha-D-galactosamine:polypeptide N-acetylgalactosaminyltransferase 7 (GALNT7), neuronal cell adhesion molecule (NRCAM), pleckstrin and Sec7 domain containing 3 (PSD3), retinoid X receptor, gamma (RXRG), and neurotrophic tyrosine kinase, receptor, type 3 (NTRK3). The most significantly downregulated genes in FVPTCs include DEP domain containing 6 (DEPDC6), glutamate receptor interacting protein 1 (GRIP1), G protein-coupled receptor 155 (GPR155), interaction protein for cytohesin exchange factors 1 (IPCEF1), and dual-specificity tyrosine-(Y)-phosphorylation regulated kinase 4 (DYRK4).
Conclusions: This is one of the first studies using high-density expression arrays to compare expression profiles between FAs and FVPTCs. Some of the newly identified and differentially expressed genes shall be assessed further for their ability to serve as diagnostic biomarkers and may help to better distinguish FAs from FVPTCs.

608 Prevalence of Micropapillary/Hobnail Pattern in Papillary Thyroid Carcinoma: A Possible Manifestation of High Grade Transformation

AM Amacher, B Goyal, J Lewis, S El-Mofty, R Chernock. Washington University, St. Louis, MO.
Background: Micropapillary/hobnail pattern is a recently described variant of papillary thyroid carcinoma (PTC) that behaves more aggressively than classical PTC, even when present only as a minor component. This pattern is characterized by the presence of micropapillae lacking fibrovascular cores and surrounded by a clear halo, as well as cellular discohesion and hobnailing. Past reports describing this variant have focused on primary tumors and have excluded all recognized variants of PTC as well as poorly differentiated/anaplastic thyroid carcinomas from analysis. The aim of this study was to evaluate the frequency of micropapillary/hobnail pattern in association with well-differentiated PTC (including recognized variants), poorly differentiated (PDCa) and anaplastic thyroid carcinomas (ATCs) in both primary and metastatic tumors.
Design: Cases of primary and/or metastatic PTC from a 5-year period (2007-2011) and all available ATCs and PDCas (1989-2011) were reviewed for at least 10% micropapillary/hobnail features. Clinical follow-up information was obtained by chart review.
Results: A total of 478 PTC (516 cases), 26 ATC and 18 PDCa patients were identified. Six PTCs patients (1.3%) had micropapillary/hobnail features. The median clinical follow-up time was 28.7 months. For PDca and ATC patients, 22% (4 of 18) and 3.8% (1 of 26) had micropapillary/hobnail features, respectively. The histopathologic and clinical features are summarized in Tables 1 and 2.

PTC Micropapillary/Hobnail Cases

Case	Histologic Variant	Primary, % MP	Metastasis, % MP	Age	Sex	Stage	Patient Status
1	Classical	10	30	23	M	I	AWD
2	Tall/columnar cell	NA	10	37	M	I	DWD (103 months following diagnosis)
3	Classical	NA	20	22	F	I	AWoD
4	Tall cell	NA	10	58	M	IVa	Alive with suspicion for recurrence
5	Classical	30	0	63	F	IVa	AWoD
6	Classical (primary), Solid (metastases)	0	40	67	M	IVa	DWD (11 months following diagnosis)

AWD: Alive with disease; NA: not available; DWD: Died with disease; AWoD: Alive without disease

Micropapillary/hobnail PDCa and ATC Cases

Case	Histologic Variant	Primary, % MP	Metastasis, % MP	Age	Sex
1	PDCa	>90	Present	62	F
2	PDCa with focal classical PTC	NA	10	76	F
3	Classical (primary), PDCa and PTC with tall/columnar cell (metastases)	0	10	50	M
4	PDCa	NA	50-60	76	M
5	ATC	10	10	46	M

NA: Not available

Conclusions: Micropapillary/hobnail pattern is more commonly associated with PDCa than well-differentiated PTC. This suggests that micropapillary pattern may be a manifestation of higher grade transformation.

609 Molecular Characterization of 48 False Negative Cases of Thyroid FNA out of 1286 Thyroid Carcinomas from a Single Institution

F Basolo, A Proietti, N Borrelli, R Giannini, F Quilici, L Torregrossa, R Romani, G Scuotri. University of Pisa, Pisa, Italy; Azienda Ospedaliero Universitaria Pisana, Pisa, Italy.
Background: Fine-needle aspiration (FNA) has been widely accepted as a cornerstone in the preoperative assessment of thyroid nodule, but the FNA accuracy remains controversial across differential studies.
Design: A retrospective review of prospectively collected data of 1286 consecutive patients with thyroid cancer who underwent thyroidectomy from March 2010 to December 2011 was performed. 1166 were papillary carcinoma (90.7%), 74 were follicular carcinoma (5.7%), 41 were medullary carcinoma (3.2%) and 5 were anaplastic carcinoma (0.4%). All patients received a preoperative FNA and were categorized into groups according to FNA results as malignant, inadequate, benign and indeterminate. In the indeterminate group were included follicular neoplasms, oxyphilic neoplasms and suspicion of thyroid cancer. All cases were reviewed and re-categorized. Malignant FNA cases were 321 (25%), indeterminate were 861 (67%), benign FNA were 48 (3.7%) and inadequate were 56 (4.3%). False negative rate was assessed (48/1286; 3.7%).
Results: Molecular testing for somatic mutation of BRAF, NRAS and HRAS was conducted in the false negative cases of papillary thyroid cancer (PTC) (38/1166; 3.2%). We found five PTCs mutated for BRAF, 3 V600E mutations and two K601E mutations. All V600E mutated cases were classical variants, whereas all K601E mutated cases were follicular variants. Moreover we found eleven NRAS Q61R mutated cases, 2 classical variants and 9 follicular variants. HRAS mutated cases were five, all of that were follicular variants. No KRAS mutated cases were found.
Conclusions: Genetic testing for somatic mutations in thyroid FNA biopsy samples is feasible and could be an important support to improve the accuracy of thyroid fine-needle aspiration biopsy. The molecular analysis in benign FNA could be evaluated.

610 GATA-3 Immunohistochemistry(IHC) Staining Pattern in Parathyroid and Thyroid Tissues, Using Histology and Cytology Samples

SS Brownschidle, JM Mitchell, AB Ambaye. University of Vermont, Burlington, VT.
Background: GATA3 is one of six members of a family of zinc finger transcription factors that interact with the GATA DNA sequence. This sequence is found in regulatory regions of many genes and plays an important role in cell proliferation, development and differentiation in many different cell types. IHC for GATA3 is becoming a useful marker in the detection of urothelial and breast carcinoma as it has been found to be quite sensitive and specific. Further, it has been suggested that low GATA3 expression may correlate with poor prognosis in breast cancer. While distal renal tubules have been found to be GATA3 positive, few other normal tissues have demonstrated GATA3 immunoreactivity to date. During validation for GATA3 IHC at our institution, we found strong immunoreactivity in parathyroid tissue. Our goal was to confirm GATA3 positivity in parathyroid tissue and examine GATA3 reactivity in parathyroid adenoma, parathyroid hyperplasia, incidentally found normal parathyroid, c-cell hyperplasia of the thyroid, benign thyroid tissue, and parathyroid cytology aspirates.
Design: GATA3 IHC was performed in 48 cases, 10 cases of parathyroid adenoma,10 cases of parathyroid hyperplasia, 10 cases of normal parathyroid, 10 cases of thyroid tissue, 3 cases of c-cell hyperplasia and 5 cytology smears of parathyroid tissue.
Results: All (35/35) parathyroid histology and cytology samples showed strong diffuse positive staining for GATA3. All (10/10) thyroid and all (3/3) c-cell hyperplasia samples stained negatively. Lymphoid cells (singly and in aggregates) stained patchy positive with decreased intensity as compared to parathyroid tissue.
Conclusions: To our knowledge, GATA3 immunoreactivity has not yet been reported in parathyroid samples in the English literature. While mouse studies suggest that GATA3 activity is essential for normal parathyroid development, a literature search did not identify any reports of IHC positivity. GATA3 IHC could aid in the sometimes problematic identification of normal parathyroid tissue in small biopsies. It can also aid in distinguishing parathyroid tissue from thyroid cytologic aspirate smears. Further, knowledge of GATA3 positivity in the parathyroid may avoid pitfalls in IHC diagnosis of tumor of unknown primary.

611 Correlation of Anti-Somatostatin Receptor Subtype 2A Immunohistochemical Expression in Neuroendocrine Tumors with Preoperative In Vivo Somatostatin Receptor Scans

NA Ciomek, S Rustagi, AC Fields, R Fardanesh, JA Strauchen, CM Divino, RP Warner. Icahn School of Medicine at Mount Sinai, New York, NY.
Background: Somatostatin receptor scans are important for the staging and management of patients with neuroendocrine tumors. Quantifying somatostatin receptor subtype 2A expression by monoclonal UMB-1 immunohistochemistry (IHC) in resected tumors has been proposed in patients without preoperative scans. The correlation between UMB-

1 expression and postoperative in vitro receptor autoradiography is high. However, the correlation of UMB-1 staining with preoperative in vivo scans has not been as extensively studied.

Design: UMB-1 staining (concentration, 1:100) was performed on resected neuroendocrine tumors from 61 patients who underwent preoperative scanning. Tumor locations included small bowel (56%), pancreas (16%), and lung (10%). Immunoreactivity was semi-quantitatively assessed in the tumor cells by two blinded pathologists as follows: 0, absent; 1+, pure cytoplasmic (focal or diffuse); 2+, membranous in less than 50% of cells; and 3+, membranous in greater than 50% of cells. Nuclear medicine findings were assessed by a five-tiered grading system (0-4). Reproducibility of the histologic scoring and correlation between tumoral IHC interpretations and scan results were analyzed.

Results: The inter-rater reliability for the histologic scoring was found to be $\kappa = 1.00$ ($p < 0.001$). Overall, only 50% of stained tumor correlated with preoperative scan results. Thirty-one patients (50.8%) had absent or low IHC scores (0 or 1+) while 30 patients (49.2%) had high IHC scores (2+ or 3+). The sensitivity was 51% and the specificity was 57%. The positive and negative predictive values were 80% and 25.8%, respectively.

Conclusions: This is the second study to correlate UMB-1 staining of neuroendocrine tumors with preoperative in vivo scans. Though the interpretation of UMB-1 staining is highly reproducible, there was poor correlation between the staining and the scan results. Our specificity and positive predictive values of 57% and 80%, respectively, were lower than the previously reported values. The prior study reported a specificity of 100% and positive predicative value of 100% in 14 neuroendocrine tumors using a higher antibody concentration (1:200). The correlation, sensitivity, and negative predictive values were also significantly lower than those previously reported.

612 Retrospective Evaluation of Frozen Section Utility for Thyroid Nodules with a Prior Fine Needle Aspiration Diagnosis of Bethesda 2-5: The Weill Cornell Medical College Experience

MA Cohen, T Scognamiglio. Weill Cornell Medical College, New York, NY.

Background: Thyroid nodules are common in the population. Fine needle aspiration (FNA) is widely used in the preoperative analysis of thyroid nodules and is a cost effective and accurate method although limitations do exist. The use of intraoperative frozen (IOF) section for thyroid nodules has been debated in the literature with many studies supporting its lack of utility. We retrospectively reviewed the contribution of IOF section in the evaluation of thyroid nodules for which there was a Bethesda diagnosis of 2-5.

Design: The surgical and cytopathology files at Weill Cornell Medical College were searched (January 2008-May 2013). A total of 429 thyroid specimens were identified for which both an FNA and subsequent IOF section was performed. The FNA was correlated with the locations of the resected nodule and the nodule frozen for intraoperative diagnosis. The results of the FNA were compared to the IOF section diagnosis and final diagnosis (FD). Of the 429 cases, the FNA diagnosis was Bethesda 2: 149 cases, Bethesda 3: 170 cases, Bethesda 4: 91 cases, Bethesda 5: 19 cases.

Results: There were a total of 77 carcinomas identified on FD. The carcinomas included 63 papillary thyroid carcinomas (PTCs) (43 follicular variants, 13 classic, 3 oncocytic variants, 1 cribriform morular variant, 2 solid variants, 1 diffuse sclerosing variant), 12 follicular carcinomas, and 2 poorly differentiated carcinomas. The preoperative FNA diagnosis for these carcinomas was as follows: Bethesda 2, 11/149 (7.4%), Bethesda 3, 24/170 (14%), Bethesda 4, 26/91 (29%), Bethesda 5, 16/19 (84%). IOF section contributed to the diagnosis of malignancy in 16/429 (4%) cases: 1/149 (0.7%) Bethesda 2, 5/170 (3%) Bethesda 3, 2/91 (1.1%) Bethesda 4, and 8/19 (42%) Bethesda 5. The diagnosis in these 16 cases included 9 classic PTCs, 3 follicular variants of PTC, 1 cribriform morular variant of PTC, 1 oncocytic variant of PTC, 1 poorly differentiated carcinoma, and 1 diffuse sclerosing variant. There were no false positives on IOF section.

Conclusions: The percentage of malignant cases that were identified from Bethesda categories 2-5 on FD is similar to those previously published. In our experience, the role of IOF section is limited in the evaluation of thyroid nodules. IOF section is most useful for nodules with a preoperative FNA diagnosis of Bethesda 5 (suspicious for malignancy). The diagnosis of follicular variant of PTC is difficult on IOF section.

613 High-Grade Neuroendocrine Carcinomas Are Characterized by Marked Transcription Factor Lineage Infidelity: An Evaluation of 36 Diagnostic Markers in 83 Tumors

TW Czeczok, MP Gailey, JL Hornick, AM Bellizzi. University of Iowa, Iowa City, IA; Brigham and Women's Hospital, Boston, MA.

Background: Immunohistochemistry (IHC) for transcription factors (TFs) is widely used to assess for tumor type and site of origin. TTF1 is expressed by 90% of small cell lung carcinomas (SCLCs) but also 40% of extrapulmonary visceral small cell carcinomas (ESCC). This lack of lineage specificity may not be confined to TTF1. Anecdotally, we have often observed high-grade neuroendocrine carcinomas (NECs) to express multiple TFs, regardless of primary site of origin. As the differential diagnosis in such cases may include other high-grade tumor types (e.g., lymphoma, melanoma, sarcoma, germ cell tumor), this phenomenon is a significant potential diagnostic pitfall. We have also seen pathologists infer a site of origin based on the results of TF IHC in NECs, which is probably not appropriate. The purpose of this study is to test the hypothesis that NECs frequently express multiple TFs, which lack lineage specificity.

Design: Tissue microarrays were constructed from 40 Merkel cell carcinomas (MCCs), 24 SCLCs, and 19 ESCCs; tumors were arrayed in triplicate. IHC for 36 TFs employed in our clinical laboratories was performed: AR, brachyury, CDX2, ER, ERG, FLI1, GATA3, HNF1B, Islet 1, MiTF, MUM1, Myb, Myc, myogenin, Nkx3.1, Oct2, Oct3/4, p40, p63, PAX2, PAX5, PAX6, PAX8, PDX1, PLAG1, PR, PU.1, SALL4, SATB2, SF1, SOX2, SOX10, STAT6, TFE3, TTF1, and WT1. For the purpose of this study, any definite nuclear staining was considered positive. Kruskal-Wallis test was used to compare medians, with a $p<0.05$ considered significant.

Results: NECs expressed a median of 8 TFs (range 0-18). The MCCs, SCLCs, and ESCCs expressed a median of 9, 8.5, and 7.5 TFs, respectively (p=0.4). TFs expressed by≥20% of cases of at least 1 tumor type are presented in the Table. 8 TFs (22%) were never expressed: brachyury, ERG, HNF1B, MiTF, Oct3/4, SF1, STAT6, and TFE3.

Frequently Expressed Transcription Factors (%)

	MCC	SCLC	ESCC
AR	11	25	16
FLI1	90	88	78
GATA3	24	8	40
Islet 1	97	88	58
Myb	67	79	0
Myc	29	25	61
Oct2	12	21	17
p40	18	17	22
PAX6	78	29	26
PAX8	20	21	26
PLAG1	58	79	72
SALL4	0	4	21
SATB2	63	42	89
SOX2	100	96	89
TTF1	5	96	44

Conclusions: NECs are characterized by striking "TF lineage infidelity," expressing 8 TFs on average. Among the most commonly expressed are FLI1, Islet 1, PLAG1, SATB2, SOX2, TTF1, and Myb--the latter 2 uncommonly in MCC and ESCC, respectively. Pathologists must be aware of this phenomenon to avoid potential interpretive errors.

614 Histological Risk Classification Predicts Malignancy and Recurrence in Paragangliomas

SJ Diaz-Cano, N Talat, A Blanes, K-M Schulte. King's College Hospital, London, United Kingdom; University of Malaga School of Medicine, Malaga, Spain.

Background: Mid-term outcome information in risk stratified patient cohort is needed to inform prognosis in individual patients with paragangliomas (PGL), adjuvant therapy choice and future research. The objective is to define the outcome relevance of a novel risk stratification scheme for PGLs.

Design: A classification scheme for PGLs was devised and specimen were assessed for invasion capacity (infiltrative edges with broad fibrous bands, extra-adrenal extension [recording capsular, microscopic periadrenal and gross periadrenal], capsular and peritumoral vascular invasion [recording thin- and thick-walled blood vessels]), tumorigenic expansion (expansile nodules with diffuse areas, hypercellular homogenous areas, necrosis [recording multifocal and confluent subtypes]) and mitogenic activity (MFC/10HPF, presence of atypical mitotic figures). Patients were prospectively stratified as low risk or high risk (presence of at least one feature of invasive capacity and two features of tumorigenic expansion). Patients underwent systematic treatment and follow up for their PGLs in a tertiary referral center.

Results: The multilevel analysis based on 78 patients identified statistically significant differences in clinical and biochemical presentation between low risk and high risk patients for gender ($p<0.05$), noradrenalin (4.6±8.5 vs 11.6±16.9), dopamine (0.6±0.3 vs 1.7±2.4), size of lesion (49.8±19.5 vs 89.2±45.8) and malignancy, 0% vs 21.6% ($p<0.01$), treatment modalities for MIBG therapy, 0% vs 40.5% ($p<.0001$), MVR, 0% vs 23.3% ($p<.001$) and lymph node dissection, 13.5% vs 40.5% ($p<0.01$) and distant metastases, 0% vs 21.6% ($p<0.01$). Disease free survival was significantly lower in HR patients 0% vs 78.4% (p=0.004). Histological risk stratification predicts DFS with AUC of 0.8 (95% CI: 0.69-0.90; $p<0.01$). 7/37 patients with HR had a synchronous diagnosis of malignancy based on other criteria and 4 patients suffered local recurrence.

Conclusions: Stratification as low risk excluded a synchronous diagnosis of malignancy and disease recurrence of a follow-up interval of 1-75 months (median 12 months). A high-risk status is associated with high risk of malignancy and disease recurrence.

615 A Previously Unrecognized Major Monocytic Component of Pheochromocytoma and Paraganglioma

N Farhat, A Tischler, J Powers, D Patricia, K Pacak. Tufts Medical Center, Boston, MA; University of Texas Health Science Center, San Antonio, TX; National Institutes of Health, Bethesda, MD.

Background: In a recent tissue culture study, we observed numerous small cells accumulated in microwells containing explants of a paraganglioma (PGL). These cells were not sustentacular or mast cells since they were negative for S-100 and CD117. This study was performed to further pursue their identity.

Design: Sections from a tissue microarray representing 50 pheochromocytomas (PCCs) and sympathetic PGLs were immunohistochemically stained for CD163 to identify monocytes and for S-100 to identify sustentacular cells. Densities of monocytes and sustentacular cells/mm^2, ratios of monocytes/sustentacular cells, and patterns of monocyte distribution in all tumors represented in the microarray were analyzed for associations with tumor size, location and genotype and with patients' age or sex. Cores of the same tumor were compared to assess intratumoral heterogeneity. Immunoblots of protein from nine additional representative tumors were probed for CD163 to test whether monocytes contribute substantially to the tumor proteome.

Results: CD163-stained cells were typically small dendritic cells aligned along tumoral blood vessels, and not usually visible in H&E sections. Sustentacular cells were typically seen at the periphery of tumor cell nests or between tumor cells. Inter- and intratumoral heterogeneity was observed for numbers and ratios of both cell types. Based on pooled counts of all cores for each individual tumor, including both PCCs and PGLs, monocyte counts revealed an average of 54.07±4.8 cells/mm^2 (n=48). Counts of sustentacular

cells revealed an average of only 13.01 ±3.1 cells/mm^2 (n=52) (p<0.0001). There were no statistically significant differences associated with patients' age or sex age for any parameters studied. Expression of CD163 protein was detected in immunoblots performed on all tumors tested, including sporadic tumors and tumors with germline mutations of PCC/PGL susceptibility genes.

Conclusions: We describe a previously unrecognized population of monocytic cells in PCCs and PGLs. Although sustentacular cells are generally recognized as a common component of these tumors, dendritic monocytes (CD163 positive cells) are more numerous. These cells typically align along small tumor blood vessels. They contribute to the tumor proteome and may have implications on tumor biology. No identifiable correlations existed between the presence of these cells with any clinical characteristics of the tumors in the present study.

616 Invasive Status Rather Than Nuclear Features Correlate with Outcome in Encapsulated Follicular Tumors: A Comparative Analysis of Encapsulated Papillary Thyroid Carcinoma Follicular Variant, Encapsulated Follicular Carcinoma and Follicular Adenoma

I Ganly, L Wang, RM Tuttle, V Cerioni, R Harach, R Ghossein. Memorial Sloan-Kettering Cancer Center, New York, NY; Dr. A. Oñativia Hospital, Salta, Argentina.

Background: The prognosis of the encapsulated follicular variant of papillary thyroid carcinoma (EFVPTC) and its relationship to encapsulated follicular carcinoma (EFC) and follicular adenoma (FA) in the classification of thyroid tumors is subject to continuous controversy.

Design: All EFVPTC, EFC and FA identified at a single institution between 1981 and 2003 were analyzed. A cohort of FA from a different hospital was also examined. Subcentimeter tumors and multicentric carcinomas were excluded.

Results: 153 patients satisfied the inclusion criteria (86 EFVPTC, 15 EFC and 52 FA). Non-invasive EFVPTC patients (n=60) were older, had smaller tumor and were more often treated by total thyroidectomy than their FA counterparts (p<0.01). Similar to FA, over a median follow up of 5.9 years, none of the non-invasive EFVPTC had lymph node (LN) metastasis, recurred, was alive with disease (AWD) at follow up (FU) or died of disease (DOD). Furthermore, with a median FU of 5.7 years, none of 43 non-invasive EFVPTC with no radioactive iodine (RAI) therapy recurred or harbored LN metastasis. In contrast, 4 (15%) of 26 invasive EFVPTC and 1 (7%) of 15 EFC had an adverse outcome (p=0.6) (Median FU: Invasive EFVPTC: 6.3 years; EFC: 5 years). There was no significant difference in metastatic LN rate between invasive EFVPTC (1/26, 4%) and EFC (0/15) (p=1) as well as no statistical difference in the rates of RAI therapy, extent of surgery, degree of capsular or vascular invasion (VI) (p>0.1). Four (15%) of 26 invasive EFVPTC developed distant metastasis (all at presentation) and 1 (7%) of 15 EFC recurred distantly (p=0.6). Of the 4 invasive EFVPTC with adverse outcome (2 AWD, 2 DOD), all had very high serum thyroglobulin (TGB), 2 had focal capsular invasion (CI) only and 2 extensive VI. The EFC who failed therapy was AWD at last FU and had focal CI and focal VI.

Conclusions: 1) Non-invasive EFVPTC seem to have a behavior similar to FA while invasive EFVPTC recur and spread like EFC. Thus, invasion rather than nuclear features drives outcome in encapsulated follicular tumors.2) EFVPTC who fail therapy seem to have aggressive clinical features at presentation in the form of distant metastasis and high serum TGB 3) Non-invasive EFVPTC should be treated in a conservative manner sparing the patients unnecessary RAI therapy. 4) The position of the EFVPTC in the classification of thyroid neoplasia should be re-considered.

617 The Molecular Characterization of Pediatric Papillary Thyroid Carcinoma

RJ Gertz, YE Nikiforov, WM Rehrauer, C Zhang, RV Lloyd. University of Wisconsin-Madison, Madison, WI; University of Pittsburgh, Pittsburgh, PA.

Background: Papillary thyroid carcinoma is an uncommon entity in the pediatric population. A limited number of studies have examined genetic mutations affecting the mitogen-activated protein kinase (MAPK) pathway in the pediatric population. We examine mutations affecting this pathway in papillary thyroid carcinoma in our pediatric population and compared the *BRAF* V600E mutations rates in pediatric and adult papillary thyroid carcinomas.

Design: Thirteen pediatric patients and 64 adult patients with papillary thyroid carcinoma were compared for the *BRAF* V600E mutation using PCR and sequencing. Additionally, we examined the rate of *RAS* point mutations using PCR and rearrangements of *RET*/*PTC1* and *RET*/*PTC3* in the pediatric group using FISH. Clinical and histological data were compared as well.

Results: The V600E mutation in *BRAF* was identified in 4 pediatric patients (31%) and 43 adult patients (67%), which was a significant difference (using Fisher's exact test P=0.026). Among the mutations, we identified a rare 3 base pair deletion mutation (c.1799_1801delTGA) in a papillary thyroid carcinoma in an 18-year old female. Mutations in *RAS* were not seen in any pediatric tumors. One tumor with a *RET*/*PTC1* and another with *RET*/*PTC3* were identified in the pediatric population (15.4%).

Conclusions: The rate of the *BRAF* V600E mutation in the pediatric population is significantly lower than that seen in the adult population. Mutations in *RAS* genes are uncommon in the pediatric population. Rearrangements *RET*/*PTC1* and *RET*/*PTC3* represent a minority of pediatric tumors. Papillary thyroid carcinomas have distinct tumor genetics in pediatric and adult populations.

618 Genomic Characterization of Adrenal Cortical Neoplasms (Carcinoma, Borderline Tumor and Adenoma) by Targeted Next Generation Sequencing: A Mutational and Copy Number Analysis

A Gopalan, H Won, G Nanjangud, A Gandhi, Y-B Chen, HA Al-Ahmadie, SW Fine, MF Berger, SK Tickoo, VE Reuter. Memorial Sloan-Kettering Cancer Center, New York, NY.

Background: Adrenal Cortical Carcinoma (ACC) is an aggressive and rare cancer with low survival rates due to advanced stage at presentation and limited availability of effective treatment. Expanded molecular discovery efforts to identify novel, actionable targets are necessary. Given the frequent difficulty in distinguishing benign from malignant tumors by histopathologic evaluation alone, there is also a need to identify genomic markers that aid in diagnosis and prognosis.

Design: Fresh frozen (FF) and Formalin Fixed Paraffin Embedded (FFPE) samples from a total of 18 Adrenal Cortical carcinoma (ACC), 7 Borderline tumors (BT) and 6 adenomas (AA), including 3 oncocytic adenomas, were included for targeted exon sequencing of 300 key cancer related genes. Tumors were classified by using Weiss criteria. FISH assay for validation of TERT gene amplification was performed on 10 samples.

Results: Sequencing revealed an overall low background mutation rate in ACC. There were 43 mutations overall: 26 in ACC, 11 in BT and 6 in AA. Recurrent mutations in ACC were seen in 5 genes: *TP53* (33%), *CTNNB1* (22%), *APC* (11%), *CHEK2* (11%) and *ATRX* (11%). The majority (16/18; 89%) of ACC had at least one mutation, including missense, nonsense and frameshift deletions. The most significant finding in terms of copy number aberrations was the presence of recurrent *TERT* gene amplifications in 4 of 10 FF samples and 3 of 8 FFPE samples of ACC. Two of the seven BT also showed low level *TERT* gene amplification. None of the AA showed this finding. Overall, AA and BT had relatively quiet genomes. FISH for the *TERT* gene was confirmatory in all 9 cases with increased *TERT* gene copy number, with either amplification (>10 copies of *TERT*) or high-level polysomy (6-10 copies of *TERT*). Tumors frequently exhibited a heterogeneous pattern on FISH. The 4 patients with ACC and high level *TERT* amplification on sequencing were either dead of disease (1) or had metastatic disease either at presentation or early in their disease course. Other significant but non-recurrent copy number abnormalities in ACC include high level amplification of *CDK6*, *CDK4*, *MDM6* and amplification of *FGFR4*.

Conclusions: The overall mutation rate in adrenal cortical carcinoma is low, with *TP53* and *CTNNB1* being the most frequently mutated genes. Copy number aberrations, in contrast, are more frequent in carcinoma as compared to borderline tumor and adenoma. Recurrent amplification of the *TERT* gene is present in nearly 40% of adrenal cortical carcinoma, and is absent in adenoma.

619 In Situ Hybridization Analysis of MiR-146b-5p and MiR-21 Expression in Thyroid Carcinoma and Prognostic Implications

Z Guo, H Hardin, S Asioli, A Righi, F Maletta, A Sapino, RV Lloyd. University of Wisconsin School of Medicine and Public Health, Madison, WI; University of Turin, Turin, Italy.

Background: MiR-146b-5p and miR-21 deregulation has been associated with progression and metastasis of thyroid cancers. However the utility of in situ hybridization (ISH) to determine the cellular localization and prognostic significance of miR-146b-5p and miR-21 expression has not been previously analyzed. We examined the expression of miR-146b-5p and miR-21 by ISH and by qRT-PCR in benign thyroid tissues and thyroid carcinomas.

Design: Anaplastic thyroid carcinomas (ATC, n=35), poorly differentiated thyroid carcinomas (PDTC, n=21), papillary thyroid carcinomas (PTC, n=58), follicular carcinomas (FTC, n=28), follicular adenomas (FA, n=32), nodular goiters (NG, n=10) and normal thyroids (NT, n=10) were studied by in situ hybridization (ISH) using formalin-fixed paraffin-embedded tissue microarrays (TMAs) with probe labeled at both 3' and 5' end with digoxigenin. ISH was scored based on intensity of stained cells. The association with miR-146b-5p and miR-21 with clinical feature and prognostic factors were analyzed.MiR-146b-5p and miR-21 expression in thyroid cancers were also analyzed by qRT-PCR.

Results: MiR-146b-5p was overexpressed in 37 out of 58 (64%) PTCs. PTC cases with higher expression of miR-146b-5p had significantly poorer disease-free survival rates. MiR-21 was overexpressed in 29 out of 35 (83%) ATCs and 4 out of 21 (19%) PDTCs, while miR-21 was overexpressed in 32 out of 58 (55%) PTCs. PTC cases with positive expression of miR-21 had significantly poorer disease-free survival rates and higher lymph node (LN) metastasis. PDTC cases with positive expression of miR-21 had significantly poorer overall survival rates. Normal thyroid tissues and most of benign goiter were negative for miR-146b-5p and miR-21. QRT-PCR analysis supported the ISH data.

Conclusions: MiR-146b-5p is mainly expressed in PTC and is not expressed in most FTC, PDTC and ATC. Thus it may serve as a useful prognostic marker for PTC. MiR-21 is highly expressed in ATC and PTC and serves as a marker of LN metastasis in PTC. ISH is a useful method to analyze microRNA expression in formalin fixed paraffin embedded tissue.

620 Diagnostic Utility of BCL-2, CD44, and CD117 in Distinction of Well-Differentiated Neuroendocrine Tumors (WD) and High Grade Neuroendocrine Carcinomas (HG)

L Hector, L Georgia, SC Smith, MJ McFall, S Mohanty, MB Amin, ME Kahn, BL Balzer. Cedars-Sinai Medical Center, Los Angeles, CA.

Background: A number of immunohistochemical (IHC) markers have been proposed as adjuncts to aid classification of neuroendocrine tumors (NET) as WD or HG. Systematic comparisons of these markers using well characterized cohorts have been lacking, despite the importance of distinction between these groups in therapeutic

decision-making. Thus, we sought to perform a systematic, side by side evaluation of published markers, including proliferative, anti-apoptotic, adhesion, and stem cell related proteins thought to distinguish between WD and HG.

Design: To enable direct, parallel comparisons of IHC markers across WD and HG neoplasms, we constructed a tissue microarray from archival blocks of NETs from our institution (1992-present), for which classification was confirmed using standard methods. These cases incorporated 60 WD (lung, n = 26; GI, n = 22, including 20 small bowel, 1 appendix, one stomach; pancreaticobiliary, n = 12) and 26 HG (lung, n = 21; GI, n = 2, including 1 cecum and 1 stomach; pancreaticobiliary, n = 3, including two pancreas and one biliary). The IHC panel included: Ki-67, chromogranin, CD44, CD117, Bcl-2, and E-cadherin. The immunostained slides were evaluated in a semi-qualitative fashion (0 = negative; 1 = weak; 2 = moderate; 3 = strong) by two observers, with >1+ considered positive. Differences between groups were tested by the U-test and Fisher's exact test.

Results: The performance of these markers in WD and HG is summarized in Table 1. For Ki-67 index, the area under the curve of the receiver operating characteristic for discrimination between WD and HG was >0.9, P<0.01, though 8% of cases showed intermediate values 4-9. For the other binary markers the sensitivity of Bcl-2, CD44, and CD117 for HG was 81%, 86%, and 78% and specificity was 82%, 40%, and 100%, respectively. All gastrointestinal and most HG were positive for Bcl-2, CD44 and CD117. All WD including lung, gastrointestinal, and pancreaticobiliary were negative for CD117.

Conclusions: We confirm the utility of Ki-67 proliferation index as a primary diagnostic adjunct in classification of WD versus HG. For cases showing intermediate proliferation indices, particularly CD117 may provide additional support for correct classification, especially in cases of limited tissue samples.

Immunohistochemical Results

Marker	WD (% Positive)	HG (% Positive)	p value
BCL-2	18	81	0.002
CD44	60	86	0.02
CD117	0	78	<0.0001
ki-67	2 (mean)	34 (mean)	<0.0001

621 Estrogen and Progesterone Receptors Are Commonly Expressed in Paraganglioma and Normal Adrenal Cortex and Less Frequently in Pheochromocytoma

A Hsi, S Sanati. Washington University School of Medicine, St. Louis, MO.

Background: Immunohistochemical (IHC) expression of estrogen (ER) and progesterone (PR) hormone receptors have been routinely used to evaluate carcinomas of unknown primary to support a breast or gynecologic origin. However, their expressions have been well documented in various non-mammary and non-gynecologic carcinomas, including primary lung and gastrointestinal malignancies. We have encountered a case of metastatic paratracheal paraganglioma in a patient with history of paraganglioma, and remote history of ductal carcinoma in situ (DCIS), in which the mass was originally misdiagnosed as metastatic breast carcinoma partially based on ER and PR positivity of the tumor. Since ER and PR expressions in adrenal medullary and paraganglial tumors are not well documented in literature, the purpose of this study was to examine the expressions of ER and PR in normal adrenal gland, pheochromocytoma, and paraganglioma.

Design: We performed a retrospective search of our Surgical Pathology files from 2007 to 2012 and identified 51 consecutive cases of paraganglioma and 45 consecutive cases of pheochromocytoma (43 of which had attached normal adrenal glands) for ER and PR IHC staining. The staining was scored using the Allred score (score range: 0-8; positive result defined as score of≥3).

Results: In normal adrenal glands, ER expression was seen in 25/43 cases (58%). PR expression was seen in all 43 cases (100%). All cases with positive staining for ER and PR showed expression within the cortex only. In pheochromocytoma, 2/ 45 cases (4%) showed ER expression. PR expression was seen in 13/45 cases (29%). 15/45 cases (33%) expressed at least one hormone receptor. In paraganglioma, 8/51 cases (16%) were positive for ER staining. PR expression was seen in 24/51 cases (47%). 29/51 cases (57%) were positive for at least one hormone receptor.

	ER+ (%)	PR+ (%)	ER+ and/or PR+ (%)	ER-PR- (%)
Adrenal Cortex	25/43 (58)	43/43 (100)	43/43 (100)	0/43 (0)
Pheochromocytoma	2/45 (4)	13/45 (29)	15/45 (33)	30/45 (67)
Paraganglioma	8/51 (16)	24/51 (47)	29/51 (57)	22/51(43)

Conclusions: Adrenal cortex, pheochromocytoma, and paraganglioma frequently express ER and/or PR. Aberrant PR expression is more common than that of ER. Because of the significant rate of aberrant expressions, it is therefore important to avoid depending solely on ER and PR expressions when evaluating tumors of unknown primary, especially in patients with history of carcinoma of mammary or gynecologic primary.

622 Detection of *BRAF* V600E Mutant Protein Expression by Immunohistochemistry in Malignant and Benign Thyroid Lesions

I John, J Tull, C Maciak, S Zhang. SUNY Upstate Medical University, Syracuse, NY.

Background: *BRAF* V600E has been used as a molecular biomarker for the diagnosis and prognosis of thyroid papillary carcinoma. Immunohistochemistry (IHC) using the anti-*BRAF* V600E antibody VE1 to detect the *BRAF* V600E mutation is a novel technique that could potentially be a more rapid and cost-effective alternative to DNA molecular testing. This study aims to assess the sensitivity and specificity of IHC in detecting *BRAF* V600E mutation in thyroid lesions.

Design: Tissue microarray immunohistochemistry analysis was performed to study *BRAF* V600E protein expression in 50 thyroid lesions. These lesions consisted of 16 papillary thyroid carcinomas (PTC), 15 follicular variant of papillary carcinomas (FVPTC), 5 follicular carcinomas (FC), 9 follicular adenomas (FA) and 5 nodular hyperplasia (NH). IHC with VE1 antibody against *BRAF* V600E protein (Spring Bioscience, 1:50) was performed according to the manufacturer's instructions. The intensity of staining was graded negative (-), positive (1+ to 3+) or equivocal (+/-). 12 positive cases and 7 negative cases were subsequently tested for *BRAF* V600E by real-time PCR.

Results: 12/16 PTC (75%) and 6/15 FVPTC (40%) showed positive expression (+1 to +3). The remainder of the cases was negative (-) except for one case of FC that showed equivocal (+/-) expression. Using DNA molecular test as a gold standard, IHC with antibody VE1 had a sensitivity of 100% and specificity of 88% for detecting *BRAF* V600E mutation. The single discordant case was the FC that was equivocal (+/-) by IHC and subsequently shown to be negative for *BRAF* V600E mutation.

Conclusions: IHC with VE1 antibody against *BRAF* V600E protein is a reliable and convenient assay to predict the status of *BRAF* V600E mutation in thyroid lesions, and can serve as a surrogate for the costly and time-consuming DNA molecular test. However, for those cases with equivocal IHC intensity (+/-), further DNA-based molecular testing is warranted.

623 IgG4 Related Thyroiditis: Low Incidence of the Disease in Germany

F Jokisch, I Kleinlein, F Prasser, T Seehaus, H Fuerst, M Kremer. Staedtisches Klinikum, Muenchen, Germany; Krankenhaus Martha Maria, Muenchen, Germany; Technical University, Muenchen, Germany.

Background: IgG4-related sclerosing disease is a newly identified syndrome characterized by high serum IgG 4 levels and increased IgG4-positive plasma cells in involved organs. Recently, the fibrosing variant of Hashimoto's autoimmune disease (HT) has been described as an IgG4-related disorder in Japan. Furthermore, Riedel's thyroiditis (RT) also is thought to be part of the IgG4-related disease spectrum. The incidence of IgG4-related thyroiditis (IgG4-T) in the caucasian population of Europe is unknown. The aim of this study was to analyze the incidence of IgG4-T in a large series of HT and Riedels thyroiditis in Southern Germany.

Design: Formalin-fixed thyroid samples of 196 pts. (191 HT, and 5 RT), were analyzed morphologically (H&E, van Gieson), and immunohistochemically, using antibodies against CD138, IgG4, IgG, CD20, CD5, kappa, and lambda. Stainings were performed on an automated immunostainer and analyzed quantitatively, whereas lymphocytic infiltration and degree of fibrosis were estimated semiquantitatively. Twenty thyroid samples (goiter) served as controls. Clinical data were obtained from the clinical files.

Results: Following the published criteria for IgG4-related diseases, cases were divided on the basis of IgG4/IgG ratio of 0.4 into two groups: IgG4-related HT (24 cases, 12%) together with RT (1 case, 20%), and 171 non IgG4-T. Compared to non IgG4-T, IgG4-related HT showed a higher IgG4/IgG ratio (0.6 vs.0.1), and a higher median IgG4 count per high power field (HPF) (x40) (45,2 vs. 6,2). The group was associated with younger age (42,1 vs. 48,1 years), a lower female-to-male ratio (11:1 vs 17,5:1), and higher levels of thyroid antibodies. Histopathologically, the IgG4-related HT group revealed a storiform-type fibrosis in 91% of the cases, whereas non IgG4-T showed a dense fibrosis in 18% (p>0.000). The single case of IgG4-related RT also showed a higher median IgG4 count per HPF (56,3 vs. 14,3), and higher IgG4/IgG ratio (0.5 vs.0.2). No differences in the degree of fibrosis were noticed in this group. Obliterative phlebitis was present in all cases of RT regardless of an IgG4 association.

Conclusions: IgG4-T can be diagnosed in a subgroup of HT and RT. The incidence in Central Europe is considerably lower than in Japan. IgG4-related HT showed morphological features of the fibrous variant of HT. It remains open, whether IgG4-T is a distinct entity apart from HT and RT, or a subgroup of both entities.

624 Progesterone Receptor and Its Synthesizing Enzymes in Pancreatic Neuroendocrine Tumor

A Kasajima, S Yazdani, H Ogata, SJA Felizola, Y Miki, Y Nakamura, H Sasano. Tohoku University School of Medicine, Sendai, Miyagi, Japan.

Background: Relatively high incidence of progesterone receptors (PR) and its favourable clinical value has been reported in pancreatic neuroendocrine tumor (P-NET). Of interest, no gender differences have been reported in its expression. Therefore, intratumoral progesterone synthesis and its actions are considered to play important roles in biological behavior of P-NET, but its details have remained unknown. Therefore, in this study we examined PR and progesterone synthesizing enzymes in normal and human P-NET tissues.

Design: 63 cases (27 male, 36 female) of surgically resected P-NET tissues were studied. 15 cases of non-neoplastic pancreatic tissues were also examined. Sex-steroid hormone receptors (ERα, ERβ, PR, PR-A, PR-B) and their metabolizing enzymes (3βHSD1, 3βHSD2, P450Scc, estrogen sulfotransferase : EST, steroid salfatase : STS, aromatase) were immunohistochemically analyzed. Results were then correlated with clinicopathological factors, including WHO grade of the cases.

Results: ERα, ERβ and PR expressions were detected in 22 (35%), 60 (95%) and 44 (70%) of the cases, respectively. The status of ER isoforms immunoreactivity was not correlated with WHO grade (ERα: P=0.87, ERβ: P=0.42) , but that of PR was highest in non-neoplastic islet cells and decreased according to WHO grade of the tumor (P<0.001). In the two different PR isoforms, PR-A status was proportional to the changes of overall PR status (P=0.004), but that of PR-B was relatively low and was not correlated with WHO grade of the tumor. Among the enzymes studied, P450scc, which catalyzes the conversion of cholesterol to pregnenolon, and 3βHSD, which then catalyzes to progesterone, were detected in P-NET, but not in normal islet cells. In addition, the status of these enzymes was significantly correlated with WHO grade of the cases (P<0.001, P<0.001, respectively). EST was frequently detected (55 cases, 87%) but not correlated with any clinicopathological factors examined.

Conclusions: Between two isoforms of PR, progesterone signals through PR-A may play more important roles in progression of P-NET than those through PR-B. In addition, the

status of PR-A was correlated with the enzymes involved in intratumoral progesterone synthesis. These results also suggest that PR-A can be the prognostic marker of P-NET and also its therapeuetic target.

625 The Intercapsular Fissure Invasion Is a Predictor of Lymph Node Metastasis in T1 Papillary Thyroid Carcinoma

KB Kim, HJ Lee, DH Shin. School of Medicine, Pusan National University, Yang San, Republic of Korea.

Background: Presence of extrathyroid extension (ETE) of papillary thyroid carcinoma (PTC) is a critical factor in staging of PTC. However, the definition of minimal extrathyroidal extension is problematic and subjective. Connected to thyroid surface capsule are interlobular fibrous septa. When PTC occurs, these fibrous septa become pulled tight toward PTC as their center, making intercapsular fissures. The minimal invasion of this intercapsular space by PTC is a frequent finding.

Design: Total of consecutive 481 PTC cases which have a single mass were reviewed. ETE was divided into three subgroups. Ex0 was the cases in which PTC is confined to thyroid gland. Ex1 was defined as invasion into soft tissue of intercapsular fissure which is bounded by thyroid gland in both sides, and imaginary line connecting thyroid gland in the base line. Ex2 was PTCs infiltrating beyond smooth thyroid capsule or imaginary line of discontinuous thyroid capsule.

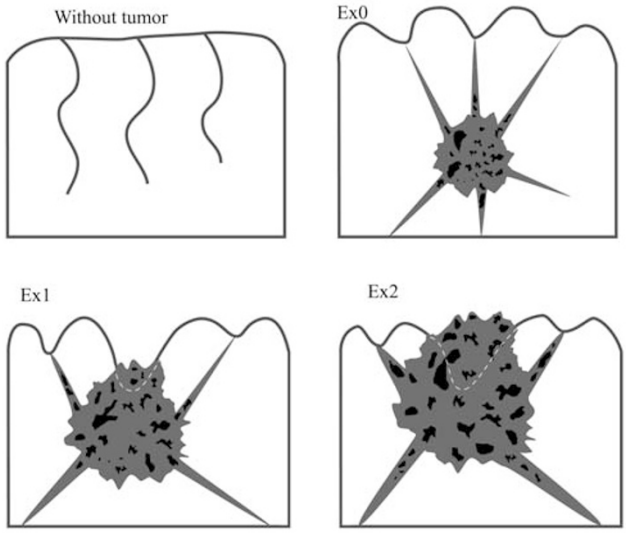

Results: Thyroid gland capsule invaginated into thyroid parenchyma and continued as fibrous septa dividing thyroid gland proper. When PTC occurs, the fibrous septa became prominent and tight, giving a characteristic stellate appearance. PTC frequently invaded these fibrous septa and septa were the main pathway of invasion into intercapsular fissure. Ex0 was 188 (38%) cases. Ex1 was 164 (34%) cases and Ex2 was 129 (27%) cases. Lymph node metastasis in each subgroup was compared to that of Ex0, of which tumor is confined to thyroid gland proper. Both of Ex1 and Ex2 subgroups were related with increased lymph node metastasis ($p<0.01$ and $p<0.01$). However, when Ex1 and Ex2 were compared to each other, no significant difference was noticed. ETE and lymph node metastasis were also evaluated according to the size of PTCs. In the first group in which PTC is less than 0.5 or 0.5cm, Ex1 showed statistically significant lymph node metastasis rate over Ex0 subgroup. The same results were seen in second and third groups.

Conclusions: Our data showed that Ex1 tumor has significantly increased lymph node metastasis rate compared to Ex0 tumor and similar metastasis rate to Ex2 tumor. Hence we think that Ex1 tumor should be regarded as having ETE. And, one of the mechanisms of lymph node metastasis in Ex1.

626 ACTH-Secreting Pancreatic Neuroendocrine Tumors Associated with Cushing's Syndrome: Clinico-Pathologic Study of 10 Cases

S La Rosa, L Albarello, A Vanoli, M Milione, O Basturk, DS Klimstra, A Watchtel, C Capella, MV Davi, A Scarpa, F Sessa. Ospedale di Circolo and University of Insubria, Varese, Italy; San Raffaele Hospital, Milan, Italy; University of Pavia, Pavia, Italy; National Institute of Cancer, Milan, Italy; Memorial Sloan-Kettering Cancer Center, New York, NY; Instituto Nacional de Enfermedades Neoplásicas, Lima, Peru; "G.B. Rossi" University Hospital, Verona, Italy; University of Verona, Verona, Italy.

Background: ACTH-secreting pancreatic neuroendocrine tumors (PanNETs), although extremely rare, are responsible for about 15% of ectopic Cushing's syndrome. About 100 cases have been reported in the English literature as case reports, but there are no studies analyzing case series, probably due to their rarity.

Design: We analyzed the clinico-pathologic features of 10 ACTH-PanNETs collected from seven different European and American Institutions.

Results: Ten patients, 6 females (mean age 33 years; range 2-60), were studied. All patients had Cushing's syndrome and two of them also presented with Zollinger-Ellison syndrome (ZES). Four patients died of disease after a mean follow-up of 68 months, while 5 patients were alive (three with clinical evident disease) after a mean follow-up of 58 months. All 8 cases for which we had the information were sporadic. The mean tumor size was 3.8 cm (range 1.5-9 cm). Most tumors showed a trabecular architecture and vascular and neural invasion. Focal necrosis was observed in one case. Three cases were NET G1, while 7 were NET G2 according to WHO criteria. Seven patients were stage III or IV, according to ENETS criteria. All tumors were positive for ACTH and 5/8 for β-endorphin. No insulin, glucagon, somatostatin, or BCL10 immunoreactivity was observed. Three cases (two of them associated with ZES) showed gastrin-positive cells, while four were CD117 positive.

Conclusions: ACTH PanNETs are generally aggressive neoplasms with metastases at the time of diagnosis and arise in patients younger than those with other PanNET types. In 20% of cases they are associated with ZES due to gastrin secretion.

627 TROP-2 Is a Potential Novel Immunomarker for Identification of Papillary Thyroid Carcinomas

H Liu, J Shi, F Lin. Geisinger Medical Center, Danville, PA.

Background: TROP-2 is a type 1 transmembrane glycoprotein and has been reported to be overexpressed in various carcinomas. Our preliminary data demonstrated TROP-2 overexpression in classic papillary thyroid carcinomas (PTC). In this study, we further investigated TROP-2 expression in a large series of benign, atypical and malignant thyroid lesions.

Design: Immunohistochemical evaluation for TROP-2 (sc-376181, Santa Cruz) was performed on 136 thyroid neoplasms on tissue microarray (TMA) sections, 61 atypical follicular lesions (AFL), and 32 normal/benign thyroid lesions (12 normal thyroid glands and 10 cases of each of lymphocytic thyroiditis and nodular goiter) on routine sections. The AFL cases included 33 PTCs (28 follicular variant and 5 classic cases; 6 of 33 cases were papillary microcarcinomas), 17 atypical follicular neoplasms (AFN), and 11 adenomatoid nodules with focal nuclear atypia (ANFNA). Immunostains for CK19, HBME-1 and galectin-3 were also performed on 61 AFL cases. Only membranous staining was considered positive. The staining intensity was graded as weak or strong. The distribution was recorded as negative (<5% of tumor cells stained), 1+ (5-25%), 2+ (26-50%), 3+ (51-75%), and 4+ (>75%).

Results: The staining results for thyroid neoplasms on TMA sections are summarized in Table 1. The staining results for AFL are summarized in Table 2. Of the 61 cases of AFL, 70% (23/33) of the PTCs were positive for TROP-2, with diffuse positivity (3+ or 4+) in 83% (19/23) of the positive cases, whereas all 11 AFN and 17 ANFNA cases were negative for TROP-2. Normal thyroid glands and 20 cases of benign thyroid lesions were also negative for TROP-2.

Table 1. TROP-2 Expression in 136 Cases of Thyroid Neoplasms

Diagnosis	1+	2+	3+	4+	Total positive cases (%)
PTC (n=48)	5	10	18	10	43 (90%)
FA (n=51)	0	0	0	0	0
FC (n=37)	0	0	0	0	0

FA: follicular adenocarcinoma; FC: follicular carcinoma

Table 2. TROP-2 Expression in 61 Cases of AFL

Diagnosis (n)	TROP-2 (%)	CK19 (%)	HBME-2 (%)	Galectin-3 (%)
PTC (n=33)	23 (70%)	22 (67%)	33 (100%)	33 (100%)
AFN (n=11)	0 (0%)	2 (18%)	9 (82%)	8 (73%)
ANFNA (n=17)	0 (0%)	3 (18%)	7 (41%)	6 (35%)

Conclusions: Our data suggest that TROP-2 is a potential novel immunomarker for identifying both classic and follicular variant papillary carcinomas. It appears to be a more specific marker than three traditional markers (CK19, HMBE-1 and galectin-3) based on this study. Additional studies with a large number of difficult cases from multiple institutions are warranted to substantiate the current findings.

628 Diagnostic Utility of SATB2 in Determining the Site of Origin of Well-Differentiated Neuroendocrine Tumors

H Lugo, M McFall, G Liles, S Mohanty, F Chung, X Yuan, MB Amin, B Balzer, D Dhall. Cedars-Sinai Medical Center, Los Angeles, CA.

Background: Determining the site of origin of a metastatic, well-differentiated, neuroendocrine tumor (WDNET) can be challenging and has prognostic and therapeutic significance. TTF1 and CDX2 are established markers for pulmonary and gastrointestinal (GI) origin, respectively. More recently, PAX6 and PAX8 are described as pancreatic markers. Although these immunohistochemical (IHC) stains are helpful in suggesting the primary site, the staining patterns are not absolutely specific. We sought to test the diagnostic utility of SATB2, a relatively novel transcriptional network regulating nuclear matrix protein involved in the embryogenesis of the skeletal system and colon, in WDNETs. We also compared SATB2 with other well-established site associated markers in WDNETs.

Design: A paraffin tissue microarray was constructed from 60 archival cases of WDNETs (lung, n = 26; GI, n = 22, including 20 small bowel, 1 appendix, one stomach; pancreas, n = 12). The IHC panel included: SATB2 and other lineage-associated transcription factors (ISL1, PAX8, PAX6, TTF1, and CDX2). The immunostained slides were evaluated in a semi-qualitative fashion (0 = no staining; 1 = weak staining; 2 = moderate staining; 3 = strong staining).

Results: The results of the key IHC markers are listed below in table 1.

The results of the key IHC markers in WDNET

IHC Markers	GI (n=22) N (%)	Pancreas (n=12) N (%)	Lung (n=26) N (%)
CDX2	21 (95)	3 (25)	0
SATB2	14 (64)	0	6 (23)
TTF1	0	0	5 (19)
ISL1	0	9 (75)	0
PAX6	0	8 (67)	0
PAX8	0	4 (33)	1 (4)

The sensitivities of CDX2 and SATB2 for GI WDNETs (particularly small bowel) are 95% and 64%, respectively, and the specificities of CDX2 and SATB2 are 92% and 84%, respectively. In GI WDNETs, the staining intensity of CDX2 is much stronger (most with 3+ staining) compared to SATB2 (most with 1+ staining). One case of appendix

NET is positive for SATB2 and CDX2, and the gastric NET is negative for both. All the pancreatic NETs, including three cases which are positive for CDX2, are negative for SATB2. However, two of three CDX2 positive pancreatic cases are also positive for either PAX6, PAX8, and ISL1. Two of 6 SATB2 lung NETs were positive for TTF1.
Conclusions: SATB2 is expressed in both GI and, less frequently in pulmonary WDNET. Though less sensitive for GI WDNET's, SATB2 is negative in the pancreatic cases tested in this series. SATB2 may therefore complement the panel of TTF-1, CDX2, PAX6, PAX8 and ISL1 in determining the site of origin of a WDNET when the differential diagnosis of the primary site is between pancreatic and GI WDNETs.

629 DAXX and/or ATRX Loss Defines Chromosomal Instability and Poor Outcome in Pancreatic NET

I Marinoni, AM Schmitt, E Vassella, M Dettmer, T Rudolph, V Banz, F Hunger, S Pasquinelli, E-JM Speel, A Perren. University of Bern, Bern, Switzerland; Inselspital University Hospital Bern, Bern, Switzerland; Maastricht University Medical Center, Maastricht, Netherlands.

Background: Sporadic pancreatic neuroendocrine tumors (pNETs) are rare and genetically heterogeneous. Chromosomal instability (CIN) has been reported in pNETs with poor outcome. Yet, no specific genetic background has been associated to CIN and the causes are still elusive. Recently, whole exome sequencing revealed mutations in *DAXX* (Death domain associated protein gene) and/or *ATRX (*ATR-X gene*)* in 40% of pNETs. Both genes encode for proteins involved in the H3.3 deposition and chromatin remodeling. Interestingly, *DAXX* and/or *ATRX* mutations in pNETs are associated with Alternative Lengthening of Telomeres (ALT) activation, a telomerase independent mechanism for telomeres length maintenance. The aim of the study was to assess whether DAXX and ATRX loss and consequent ALT activation is related to CIN in pNETs and if DAXX and ATRX loss defines a clinically relevant molecular subtype.
Design: We performed DAXX and ATRX IHC and telomeric FISH on two different pNET collectives comprising a total of 243 well differentiated primary pNET. Of these, follow up data was available for 149 patients. We correlated loss of DAXX, ATRX expression and ALT activation with CGH (Comparative Genomic Hybridization) array data as well as with clinico-pathological characteristics, tumor relapse and survival data.
Results: We show that DAXX and/or ATRX protein loss and ALT activation is associated with CIN in pNETs (p=0.036 and p=0.0095). Furthermore, loss of DAXX and/or ATRX expression correlates with tumor stage and metastasis and predicts both shortened relapse-free survival (p=0.0001) and decreased tumor specific survival (p=0.0019).
Conclusions: Our findings indicate for the first time that DAXX and/or ATRX loss might be the reason for CIN in pNETs and that predicts poor outcome. These results support the hypothesis that DAXX and ATRX negative tumors represent a specific biological subtype of pNETs with distinct molecular characteristics, and pave the way for the identification of new potential targets leading to CIN in pNETs.

630 CD5 in Squamoid Morulae of Cribriform-Morular Variant Papillary Thyroid Carcinoma: A Possible Link to Divergent Thymic Differentiation

O Mete, V Nose, SL Asa. University Health Network, Toronto, ON, Canada; Massachusetts General Hospital, Boston, MA.

Background: Cribriform architecture and squamous metaplasia are features of papillary thyroid carcinoma (PTC), however, recognition of the cribriform-morular variant of PTC is of clinical importance; it is found in patients with germline mutations of the *APC* gene who have familial predisposition to develop polyposis coli. Rarely, sporadic mutation of *APC* in these tumors is unassociated with germline or familial disease. In addition to diagnostic nuclear features of PTC, a complex cribriform architecture and the formation of squamoid morulae, nuclear and cytoplasmic localization of beta-catenin is regarded as a characteristic of these rare neoplasms. In this study, we investigated the immunoprofile of squamoid morulae of cribriform-morular PTC to clarify their cellular differentiation.
Design: Nine cases of cribriform-morular PTC with nuclear and cytoplasmic beta-catenin expression were included in this cohort. One representative block from each tumor was subjected to a panel of immunohistochemical analyses using antibodies against TTF-1, thyroglobulin, monoclonal carcinoembryonic antigen (mCEA), high molecular weight keratin (CK5), p63 and CD5.
Results: The cribriform areas were positive for TTF-1 and thyroglobulin with variable intensity; they were negative for CD5, p63 and mCEA. In contrast, the squamoid morules were diffusely positive for CD5 and were variably positive for TTF-1 while thyroglobulin and p63 were negative. CK5 and mCEA were also negative in morulae.
Conclusions: Cribriform-morular variant PTCs exhibit variable amounts of squamoid morular differentiation. CD5 is expressed mainly in lymphocytes and thymic epithelial cells; intrathyroidal thymoma, thymic carcinoma and carcinoma showing thymic elements (CASTLE) are positive for CD5. TTF-1 is also variably expressed in thymic epithelium including thymomas. Our findings suggest that CD5-positive squamoid morulae in this rare variant of PTC may represent divergent thymic epithelial differentiation rather than squamous metaplasia of thyroid follicular epithelium as previously proposed.

631 Biomarkers of Adrenal Cortical Carcinoma

O Mete, H Gucer, M Kefeli, SL Asa. University Health Network, Toronto, ON, Canada.

Background: The distinction of non-invasive low-grade adrenal cortical carcinoma from adrenal cortical adenoma with atypical features is a challenge. While many algorithms and scoring schemes have been defined, they all have limitations. Transcriptome studies have suggested potential biomarkers of malignancy. We investigated potential biomarkers of malignancy including proteins involved in telomere regulation, DNA damage repair, and pseudohypoxia pathway in a series of adrenal cortical neoplasms.
Design: We constructed a tissue microarray of 45 adrenal cortical carcinomas and 50 adenomas and stained the slides for IGF-2, BUB1, PBK, beta-catenin, p53, MIB-1, DAXX, ATRX, and SDHB. The reticulin network was assessed with the Gordon-Sweet silver stain and scored as 1-4. Individual cores were scored by multiplying the percent positive cells by intensity (1-3), and each tumor received an average score (max: 300) for IGF-2, BUB1, and PBK. Complete loss of DAXX, ATRX, and SDHB, and presence of nuclear beta-catenin, along with the labeling index (LI) of p53 and MIB-1 were recorded.
Results: Expression of IGF-2, BUB1, PBK were significantly higher in carcinomas (IGF2: 97%, score 247.95; BUB1: 60%, score 26.47; PBK: 47%, score 14.80) than in adenomas (IGF2: 32%, score 6.40; BUB1: 4%, score 0.12; PBK: 8%, score 0.28) (p: 0.0001; p: 0.0002; p: 0. 0018). Loss of nuclear beta-catenin was only seen in 6 carcinomas (p: 0.0053). The mean MIB-1 and p53 LIs were significantly higher in carcinomas (MIB-1: 7.82%, SD: 13.0; p53: 19.64%, SD: 29.44) than in adenomas (MIB-1: 1.5%, SD: 0.95; p53: 4.44, SD: 6.22) (p: 0.0009; p: 0.0006). DAXX and ATRX were lost in 18 and 23 of 45 carcinomas respectively; loss was also seen in 6 and 8 adenomas respectively but the difference was statistically significant (p: 0.0011; p: 0.0001). Loss of reticulin network more than 50% was seen in the majority of carcinomas (p: 0.0001). There was no loss of SDHB in any tumor. The combination of markers proved malignancy in 44 of 45 carcinomas and the one negative tumor remains clinically unproven as malignant.
Conclusions: Our data suggest that the immunohistochemical diagnosis of adrenal cortical carcinoma can be rendered using a panel of biomarkers including IGF-2, BUB1, PBK, beta-catenin, p53, and Ki-67, and with the assessment of reticulin network. Positivity for IGF2 is common; p53 and Ki67 LIs, nuclear beta-catenin expression and positivity for BUB1 and PBK are more variable. PBK expression correlates with Ki67, p53, and BUB1 expression, indicating proliferative activity of the tumor. The DAXX/ATRX telomere regulation pathway is also implicated in adrenal cortical tumorigenesis.

632 Paired Related Homeobox 1 (PRRX1) Is Associated with Epithelial-Mesenchymal Transition (EMT) in Thyroid Tumors

C Montemayor Garcia, Z Guo, H Hardin, D Buehler, V Nose, S Asioli, A Righi, F Maletta, A Sapino, H Chen, RV Lloyd. University of Wisconsin School of Medicne and Public Health, Madison, WI; Massachussetts General Hospital, Boston, MA; University of Turin, Turin, Italy.

Background: PRRX1 is a newly identified transcription factor that induces EMT in various neoplasms. We examined the expression of PRRX1 in benign thyroid tissues and thyroid carcinomas and in a cultured thyroid cell line, PTC1, after induction of EMT with TGFβ1.
Design: Anaplastic thyroid carcinomas (ATC, n=35), poorly differentiated thyroid carcinomas (n=21), papillary thyroid carcinomas (PTC, n=58), follicular carcinomas (n=28), follicular adenomas (n=32), nodular goiters (n=10) and normal thyroids (n=10) were analyzed by immunohistochemistry (IHC) using formalin-fixed paraffin-embedded tissue microarrays (TMAs). IHC was scored based on the percentage and intensity of stained cells. The association of PRRX1 expression with clinical features and prognostic factors was also analyzed. Whole sections of PTCs (n=20) were also analyzed by IHC for PRRX1 expression. The TPC1 cell line was treated with TGFβ1 to induce EMT and PRRX1 was analyzed by qRT-PCR.
Results: PRRX1 showed nuclear expression mostly in ATCs (54%) in the TMAs compared to all other groups (p<0.005).Whole sections of PTCs were positive in 2/5 (40%) cases of the hobnail variant of PTCs while conventional PTCs (n=10) and tall cell variant of PTC (n=5) were all negative. Positive expression of PRRX1 correlated with patient age, lymph node metastasis, tumor size and extrathyroidal extension. Moreover PRRX1 was related to poorer survival in patients with thyroid cancer. After TGFβ1 induction of EMT, there was a 10 to 20 fold increase in PRRX1 mRNA expression over a 30 day period.
Conclusions: The PRRX1 transcription factor is expressed mainly in ATC and in some aggressive variants of PTCs such as the hobnail variant in primary thyroid tumors. Induction of EMT in vitro by TGFβ1 treatment leads to increased expression of PRRX1.

633 VE1 Antibody Expression in Normal Anterior Pituitary and Adrenal Cortex without Detectable *BRAF* V600E Mutations

DA Mordes, K Lynch, S Campbell, D Dias-Santagata, V Nose, DN Louis, MP Hoang. Massachusetts General Hospital, Boston, MA.

Background: *BRAF* has been found to be mutated in a variety of human tumors. The VE1 monoclonal antibody was developed to recognize the most common activating mutation in *BRAF* using immunohistochemistry on formalin-fixed paraffin-embedded tissue.
Design: VE1 antibody staining and SNaPshot BRAF V600E genotyping were performed on archival, formalin-fixed, paraffin-embedded materials of postmortem pituitary glands, adrenocorticotropic hormone (ACTH) producing pituitary adenomas, adrenal glands, parathyroid glands, pancreas and thyroid glands.
Results: We report that the VE1 antibody stains normal anterior pituitary gland and adrenal cortex that lack detectable *BRAF* V600E mutations. Staining with the VE1 antibody was seen in the adenohypophysis and correlated well with ACTH-positive cells. There was absence of VE1 staining in the neurohypophysis. ACTH-positive cells were typically most concentrated in the central mucoid wedge and pars intermedia, and VE1 staining was strong in these regions. Moreover, VE1 staining was seen in ACTH-expressing pituitary adenomas without detectable *BRAF* mutations. There was also significant VE1 staining of the adrenal cortex but not the adrenal medulla. The strongest VE1 staining was seen in the inner segment of the zona fasciculata and to a lesser degree in the zona reticularis. On the other hand, there was no VE1 staining of parathyroid glands, pancreatic islets, or parafollicular C cells in the thyroid.
Conclusions: Overall, VE1 staining of endocrine tissues strongly suggests limitations on the use of this antibody for the detection of *BRAF* mutations.

634 Next-Generation Sequencing Panel (ThyroSeq) in Extended Mutational Profiling of Thyroid Cancer

MN Nikiforova, A Wald, S Zhong, S Roy, YE Nikiforov. University of Pittsburgh, Pittsburgh, PA.

Background: Next-generation sequencing (NGS) allows for massively parallel sequencing of the human genome and becomes a powerful tool for the detection of genetic alterations. We report here a novel targeted NGS panel (ThyroSeq) for the detection of mutations and gene fusions in thyroid cancer that can be used in clinical setting.

Design: ThyroSeq NGS panel was designed to sequence 13 thyroid cancer related genes for point mutations and for 30 types of gene fusions using next generation sequencing on Ion Torrent PGM (Life Technologies). The panel was validated on 318 samples from thyroid neoplastic and non-neoplastic nodules including tissue and FNA samples.

Results: Small amount of nucleic acids (5-10 ng) was sufficient for successful analysis of 99% of thyroid tissue and FNA samples using ThyroSeq NGS panel. The analytical accuracy for mutation detection was 100% with sensitivity of 3-5% of mutant alleles for point mutations and 1% for fusion transcripts. ThyroSeq DNA assay identified mutations in 70% of PTC, 83% of follicular variant PTC, 78% of conventional and 39% of oncocytic follicular carcinomas, 30% of poorly differentiated carcinomas, 74% of anaplastic, and 73% medullary carcinomas. In contrast, only 6% of histologically benign thyroid nodules were positive for mutations. The most common mutations detected were BRAF and RAS followed by PIK3CA, TP53, TSHR, PTEN, GNAS, CTNNB1 and RET. ThyroSeq NGS analysis identified common gene fusions including RET/PTC1, RET/PTC3, and PAX8/PPARγ, and also rare fusion types involving RET/PTC6, BRAF, NTRK1 and NTRK3 rearrangements. This method provided quantitative assessment of mutations and confirmed the clonal origin of BRAF and other mutations.

Conclusions: ThyroSeq NGS panel (i) allows testing for multiple mutations and gene fusions with high accuracy and sensitivity; (ii) requires small amount of DNA and RNA, and (iii) provides quantitative assessment of mutant alleles and fused transcripts. ThyroSeq NGS approach detects genetic alterations in a cost effective way and can be used as an ancillary diagnostic test for surgically removed and FNA samples.

635 Neuroendocrine Tumors(NET) G3 with Frequent Immunohistochemical SSTR2a Expression: Neuroendocrine Carcinomas (NEC WHO 2010) Are Not Always Large Cell or Small Cell Type. A Proposal from a Large Series of Referred Cases

RY Osamura, C Inomoto, H Kajiwara, M Matsuda. International University of Health and Welfare, Tokyo, Japan; Tokai University, School of Medicine, Kanagawa, Japan.

Background: In WHO Classification 2010, neuroendocrine tumors(NET) are subdivided into NET G1, NET G2 and NEC(large cell or small cell type) according to mitotic counts or Ki67 indices. NEC(WHO) is diagnosed when Ki67 labeling is higher than 20% Our study has indicated that not all NEC are large or small cell type and that some disclose typical "well differentiated(WD)" neuroendocrine histology. Thus terminology NET G3 has been proposed. This study is aimed at to elucidate whether NEC(WHO2010) could be further subdivided into (1)NET G3 and (2)NEC(large cell or small type) on the basis of "WD"neuroendocrine histology. Immunohistochemical detection of SSTR2a is also detected for the treatment with somatostatin analogue.

Design: Total 328 referred cases of NET/NEC were subjected to the following study. Primary and metastatic (hepatic) NET/NEC were classified according to WHO 2010. The primary NEC with >20% Ki67(MIB1, DAKO) were subdivided to NET G3 when the tumors exhibit one of the following histologic features of "WD" NET histology, i.e., ribbon-like, pseudorosette, organoid, and rosette structures. The tumors without these features are designated as NEC(small cell or large cell type). Immunohistochemical staining for SSTR2a was done by rabbit monoclonal antibody (Epitomics, Inc. USA).

Results: Proportion of NET G1, NET G2 and NEC in the primary tumors(57 cases)) were 23%, 21%, 56% . Total thirty primary NEC(WHO 2010) included four cases of pancreatic NEC and 26 cases of non-pancreatic NEC(including stomach, duodenum, rectum). Among these, three cases of pancreatic NEC and 10 cased of non pancreatic NEC were reclassified as NET G3 according to the above criteria. The other cases remained to be designated as NEC. The NET G3 cases showed average MIB1 labeling index as 52.8% and 85% of cases were positive for SSTR2a. In contrast, 17 cases of NEC(Large cell and small cell) revealed 70.8% and 30% respectively.

Conclusions: Our study indicated that NEC(WHO 2010) are not always large or small cell type and contain certain proportion of NET G3(43.3%) detected by "WD" neuroendocrine histology.The NET G3 revealed higher incidence of SSTR2a positive staining than that of NEC(large cell and small cell type) suggesting better response to somatostatin analogue therapy. The role of pathologists in the practice of this subdivision of NET G3 should be emphasized.

636 BRAF V600E in Pediatric Papillary Thyroid Carcinomas

VA Paulson, ML Hollowell, SA Huang, JA Barletta. Brigham and Women's Hospital, Boston, MA; Boston Children's Hospital, Boston, MA.

Background: In adults roughly 45% of papillary thyroid carcinomas (PTCs) harbor the *BRAF* V600E mutation. While the rate of *BRAF* mutation is thought to be lower in pediatric PTCs, the frequency has not been established. The aim of this study was to evaluate the *BRAF* V600E mutation rate in pediatric PTCs utilizing immunohistochemistry (IHC) and correlate the expression status with clinicopathologic features and outcome.

Design: We identified 26 PTCs (22 thyroidectomies and 4 lymph node resections) diagnosed between 1999 and 2013 in children 21 years of age or younger. Pathologic parameters recorded included: tumor size and multifocality, PTC type, extrathyroidal extension (ETE), lymph node (LN) status, and distant metastases. IHC for BRAF V600E (VE1) was performed. Homogeneous, strong, granular cytoplasmic staining was scored as positive (BRAF-Pos), no staining (or a weak cytoplasmic blush) was scored as negative (BRAF-Neg), and moderate, heterogeneous staining was considered equivocal. Clinical characteristics and follow-up information were obtained from electronic medical records.

Results: Our cohort included PTCs from 20 females and 6 males, with a mean age of 15 years at diagnosis (range 8-21 years). Four (15%) PTCs were BRAF-Pos, 20 (77%) were BRAF-Neg, and 2 (8%) were equivocal (one equivocal case was known to be *BRAF* wild-type by molecular analysis and was included in the BRAF-Neg group). Although patients with BRAF-Pos tumors were older than those with BRAF-Neg tumors, the difference was not significant (mean age 17 and 15 years, respectively; p=0.16). All BRAF-Pos cases were classical type PTCs, while the BRAF-Neg group included 15 classical, 5 follicular variant, and 1 diffuse sclerosing variant. There was no difference in tumor size, rate of multifocality, rate of ETE, LN status, or presence of distant metastases at diagnosis between the 2 groups. There was a trend toward a higher recurrence rate in the BRAF-Pos group (p=.0565; median follow-up period 64 months). Two (50%) patients with BRAF-Pos tumors recurred, 1 with LN metastases at 61 months and the other with pulmonary metastases at 28 months. Only 1 (5%) patient with a BRAF-Neg tumor recurred; however, this patient eventually died of disease (deceased at 200 months).

Conclusions: 15% of pediatric PTCs in our cohort were positive for BRAF V600E. There was a trend towards a higher recurrence rate in patients with BRAF-Pos tumors.

637 Spectrum of Lesions Derived from Ultimobranchial Body Occurring in the Thyroid: From Solid Cell Nests to Tumors

K Peckova, R Hamplova, M Michal, O Daum. Medical Faculty Hospital, Charles University, Plzen, Czech Republic; Panoch Hospital, Turnov, Czech Republic.

Background: There is a group of lesions in the head and neck derived from branchial arches which, when inflammed, are characterised by the formation of cysts lined by squamous or glandular epithelium and surrounded by inflammatory infiltrate. In the thyroid, ultimobranchial body derived from inferior branchial arches is a source of various structures which may cause diagnostic dilemma.

Design: Our consultation files were reviewed for cases containing pathological structures regarded to arise from ultimobranchial body. The slides stained with H&E were evaluated for ultimobranchial structures. Positive IHC reaction with antibodies against CK5/6 and CEA, and lack of expression of thyroglobulin and calcitonin were suggested to confirm the diagnosis. The specific subtype of the lesion was then determined based on histological examination of H&E stained slides.

Results: 20 cases of ultimobranchial body-derived lesions were retrieved, 19 with available clinical information (M/F = 6/13, mean age 54 years, range 36-68 years). Further clinical or histological findings were: thyrotoxicosis (2), Hashimoto thyroiditis (10), multinodular colloid goiter (1), follicular adenoma (1), papillary microcarcinoma (1), and MALT lymphoma (1). Lesions derived from ultimobrachial body were classified as follows: (hyperplastic) solid cell nests (10), solid cell nests with focal cystic change (4), cystic solid cell nests (2), branchial cleft-like cyst (3), and finally a tumor sized 15 mm composed of a part of solid cell nests appearance, a part resembling a branchial cleft cyst, and a part resembling Warthin´s tumor (1).

Conclusions: Pathological lesions derived from ultimobranchial body remnants in the thyroid gland span a wide spectrum of morphological patterns. The common denominator of these structures is that they all arise as an inflammatory process around these vestigial structures, which lead to cystic dilatation and proliferation of the epithelial component. The epithelium afterwards can become papillary, and thus acquire the features of a Warthin´s tumor. In addition to usual structures (solid cell nests with various grades of cystic transformation and branchial cleft-like cyst) we report on an exceedingly rare lesion of the thyroid probably of a branchial cleft origin, which was not published in the world literature before, and which was found to stand beyond the current WHO classification system even by a world leading expert in thyroid pathology.

638 Urinary Steroid Profiling for the Preoperative Identification of Adrenocortical Adenomas with Regression and Myelolipomatous Changes

V Perna, N Taylor, D Dworakowska, K-M Schulte, A Blanes, SJ Diaz-Cano. University Hospital, Seville, Spain; King's College Hospital, London, United Kingdom; University of Malaga School of Medicine, Malaga, Spain.

Background: Adrenocortical neoplasms are classically divided into adenomas (ACA) and carcinomas (ACC). Heterogeneous appearance and greater size are criteria to suggest malignancy, along with the urinary steroid profile (USP). The presence of regression and myelolipomatous changes in adenomas (ACA-RML) can contribute to confusion with ACC and its USP remains unknown. *Objective:* To evaluate the features of ACA-RML in comparison with other adrenocortical neoplasms.

Design: We selected consecutive ACA (11), ACA-RML (7) and ACC (13) cases for which USP analysis was performed before surgery and tissue was available for histological evaluation (King's College Hospital, 2005-2012). Cases were classified according to WHO and Armed Forces Institute of Pathology criteria. USPs were obtained by gas chromatography/mass spectrometry. Total excretion of individual steroids and indices (sums and ratios chosen to reflect steroid metabolic activity) were compared between ACA-RML, ACA, and ACC. Steroids that have proved to be useful markers of ACC were also compared empirically between groups, including tetrahydro-11-deoxycortisol, pregnene3,16,20-triols, 16a- and 21-hydroxypregnenolone and tetrahydro-11-deoxycorticosterone.

Results: In comparison with ACA, tumors in ACA-RML were significantly larger (8.5±2.4 vs. 3.5±1.0, P=0.002), presented in older patients and showed relatively higher incidence in males. Mitotic figure counts were significantly lower (0.39±0.04 vs. 0.93±0.11 in ACA, p=0.001) and revealed higher frequency of apoptotic cells (100% vs. 9% in ACA, p= 0.001). The USP of ACA-RML showed no diagnostic features of ACC, along with lower levels of DHA and DHA metabolites.

Conclusions: ACA-RML reveals distinctive histological features, and lack of USP markers of malignancy. It is important to recognize ACA-RML because its size and heterogeneous appearance raise the possibility of ACC; in this context, USP is an important tool for a correct preoperative diagnosis.

639 Multifocal Papillary Thyroid Microcarcinomas: Evaluation Via Total Tumor Diameter and Total Surface Area

J-S Pyo, JH Sohn, D-H Kim, G Kang. Kangbuk Samsung Hospital, Sungkyunkwan University School of Medicine, Seoul, Republic of Korea; Inje University Sanggye Paik Hospital, Seoul, Republic of Korea.

Background: Papillary thyroid microcarcinoma (PMC), regardless of tumor multifocality, is known to have a favorable prognosis. In multifocal PMC (mPMC), the largest tumor size is an important factor in predicting tumor behavior, but it does not fully explain all aspects of this behavior. The purpose of this study was to identify more precise predictable factors for multifocal PMC.

Design: The diameter of the dominant tumor (TD), total tumor diameter (TTD) and total surface area (TSA) were retrospectively investigated in 384 consecutively resected classical variant of PMCs. Then, we were evaluated the correlations between TTD and TSA and clinicopathological features in both multifocal and unifocal PMCs.

Results: Tumor multifocality was found in 104 cases (27.1%). Multifocal PMCs were significantly correlated with lymph node metastasis and higher tumor stage grouping ($P = 0.004$ and $P < 0.001$, respectively). TTD and TSA were significantly larger in mPMCs than in unfocal PMCs. However, largest tumor size of mPMCs correlated significantly with extrathyroidal extension ($P = 0.029$), but not with nodal metastasis ($P = 0.830$). Higher rates of nodal metastasis were found in more cases of mPMC with TSA > 3.14 cm^2 than in mPMC with TSA ≤ 3.14 cm^2 ($P = 0.038$); however, there was no significant difference between mPMC with TTD > 1.0 cm and with TTD ≤ 1.0 cm (P = 0.325).

Conclusions: These results suggest that a higher TSA, but not TTD, for mPMC is significantly correlated with lymph node metastasis. TSA could be useful in evaluating tumor behavior of mPMCs.

640 Comprehensive Genomic Profiling of Adrenal Cortical Carcinoma Reveals Actionable Genomic Alterations and New Routes to Targeted Therapies

JV Rand, MJ Presta, K Wang, CE Sheehan, GA Otto, G Palmer, R Yelenksy, D Lipson, J Chmielecki, SM Ali, D Morosini, VA Miller, PJ Stephens, JS Ross. Albany Medical College, Albany, NY; Foundation Medicine Inc, Cambridge, MA.

Background: Adrenal Cortical Carcinoma (ACC) is a rare but aggressive tumor. Complete surgical resection is the only cure, but many patients are inoperable at diagnosis and require non-curative systemic treatments which yield a low 5-year survival rate. We hypothesized that comprehensive genomic profiling of clinical ACC samples by next generation sequencing (NGS)-based genomic profiling could identify genomic-derived drug targets of therapy for patients with this aggressive form of cancer.

Design: Hybridization capture of 3,320 exons from 182 cancer-related genes and 37 introns of 14 genes commonly rearranged in cancer (previous version of the test) and 3,769 exons from 236 cancer-related genes and 47 introns of 19 genes commonly rearranged in cancer (current version of the test) was applied to≥ 50ng of DNA extracted from 25 Adrenal Cortical Carcinoma tumor specimens and sequenced to high, uniform coverage. Genomic alterations (base substitutions, small indels, rearrangements, copy number alterations) were determined and then reported for these patient samples. Actionable GA were defined as those identifying anti-cancer drugs on the market or in registered clinical trials.

Results: There were 12 female and 13 male ACC patients with a median age of 51.8 years (range 21-77 years). There were 10 Grade 3, and 15 grade 4 tumors (Fuhrman grading system). Two were Stage II, 21, were Stage III, and two were Stage IV at time of profiling. Nine ACC were primary tumors and 16 were a metastasis biopsy. A total of 63 alterations were identified with an average of 2.52 GA per tumor in the 19/25 (76%) of cases in which an alteration was identified. The most common non-actionable GA were alteration of *TP53* (36%), *CTNNB1* (16%) *MEN1* (16%) and *RB1* (8%). Thirteen of twenty five (52%) ACC had at least 1 actionable GA with an average of 1.04 actionable GA per patient (26 total) including mutation, homozygous deletion or amplification of in *NF1* (24%), *ATM* (12%), loss in *CDKN2A* (8%), *CCND2* (8%), *CDK4* (8%) with *EGFR*, *ERBB4*, *KRAS*, *MDM2*, *NRAS*, *PDGFRB*, *PIK3CA*, *PTEN*, *PTCH1* and *STK11* each altered in a single case.

Conclusions: More than half of the ACC patients in this study harbored actionable GA. Given the limited treatment options and poor prognosis of patients with locally advanced and metastatic ACC, comprehensive NGS-based genomic profiling has the potential to identify new treatment paradigms and meet an unmet clinical need for this disease.

641 Non-V600E *BRAF* Variants in Papillary Thyroid Carcinoma

K Ricci, D Chute, R Tubbs, S MacNamara, F Lacbawan. Cleveland Clinic, Cleveland, OH.

Background: Papillary thyroid carcinoma (PTC) is most frequently associated with mutations in the activation segment of BRAF, a serine/threonine kinase signaling protein. The V600E mutation is found in over 90% of PTCs with *BRAF* gene mutations and is associated with more aggressive tumors and certain morphological subtypes. We reviewed the clinical and histologic features of PTC in rare non-V600E *BRAF* variants.

Design: We performed a retrospective analysis of patients with PTC who had novel and rare mutations in Exon 15 of *BRAF*. Cases were reviewed for histologic features. Tumor DNA was extracted from formalin-fixed paraffin embedded tissue of thyroidectomy specimens. Bidirectional Sanger sequencing of *BRAF* Exon 15 was performed by the *ABI 3730 Genetic Analyzer* following targeted PCR. Mutation analysis was performed using *Qiagen BRAF RGQ PCR* assay for comparative mutation detection.

Results: We identified 4 mutations in 8 PTCs with novel or rare mutations. A novel insertion-deletion (c.1796-1805 del CAGTCAAATC ins T) was identified. We also identified 3 cases of p.K601E point mutations, 3 cases with a deletion at c.1799T_1801del TGA (p.VK600-1E), and a nonsense mutation at c.1834C>T (p.Q612X). The histologic features of each tumor are listed in Table 1. Vascular invasion, lymph node metastasis, and extrathyroidal extension were absent in all cases. The novel insertion-deletion was present in a 1.0 cm macrofollicular-variant PTC, arising in otherwise normal thyroid. The *Qiagen BRAF RGQ PCR* assay detected a *BRAF* mutation in the novel insertion-deletion case and the p.VK600-1E variant, but was negative in the other rare mutations.

Table 1: Histologic Features of BRAF Variant PTC Cases

Mutation	Size (cm)	Foci	Variant	Capsule	Invasion	Background
p.K601E c.1801A>G	3.4	4	Solid/Follicular	+	-	NH
p.K601E c.1801A>G	2.0	1	Follicular	+	-	NH
p.K601E c.1801A>G	1.1	3	Follicular	+	-	C-Cell Hyperplasia
p.VK600-1E c.1799T_1801delTGA	1.5	2	Follicular	+	+	NH
p.VK600-1E c.1799T_1801delTGA	1.1	1	Classical	-	+	NH
p.VK600-1E c.1799T_1801delTGA	0.4	3	Classical	+	+	CLT
p.Q612X c.1834C>T	0.4	3	Classical with Focal Tall Cell	-	+	NH
c.1796_1805 del CAGTCAAATC ins T	1.0	1	Macrofollicular	+	-	Normal

NH-Nodular Hyperplasia, CLT-Chronic lymphocytic thyroiditis

Conclusions: We identified a novel sequence variant in *BRAF* in a macrofollicular variant papillary thyroid carcinoma and 3 rare mutations in 7 other cases. Bidirectional Sanger sequencing is better in the identification of rare *BRAF* variants, as the *Qiagen BRAF RGQ PCR* assay only detected 2 of the 4 variants.

642 *RAS* Mutations in Medullary Thyroid Carcinoma

EM Rinehart, M Capelletti, RI Haddad, PA Janne, NG Chau, JA Barletta. Brigham and Women's Hospital, Boston, MA; Dana-Farber Cancer Institute, Boston, MA.

Background: A subset of sporadic medullary thyroid carcinomas (MTCs) harbors *RAS* mutations. The aim of this study was to evaluate the frequency of *RAS* mutations in a cohort of MTCs evaluated at our institution and correlate *RAS* mutation status with histopathologic features.

Design: We identified 31 thyroidectomies with MTC evaluated at our institution between 2000 and 2012. Pathologic parameters recorded included: tumor size and multifocality, tumor morphology, extrathyroidal extension (ETE), and lymph node (LN) status at initial resection. DNA was extracted from formalin-fixed, paraffin-embedded tumor blocks. PCR primers were designed to interrogate known mutation hot spots for *RET* (exons 8, 10, and 13-16 were evaluated; exon 11 analysis is underway) and for *HRAS*, *KRAS*, and *NRAS* (codons 12, 13, and 61 were evaluated; *NRAS* analysis performed on 17 of 31 cases to date).

Results: Our cohort included 17 females and 14 males, with a mean age of 54 years (range 28-75 years). Eight (26%) MTCs harbored *RAS* mutations, 7 (23%) harbored *RET* mutations, 1 (3%) harbored both a *RET* and *RAS* mutation, and 17 (55%) had no mutation detected. The 8 *RAS* mutations included 5 *HRAS* (all p.Gln61Arg) and 3 *KRAS* mutations (two p.Gly12Arg and one p.Gln61Arg). The one tumor that harbored both a *RAS* and *RET* mutation was *HRAS* mutant and also had *RET* p.Val804Met. MTCs with *RAS* mutations were histologically indistinguishable from MTCs with *RET* mutations, were similar in size (mean size 3.0 and 3.9 cm, respectively), and had a similar rate of multifocality (14% and 33%, respectively). While MTCs with underlying *RAS* mutations had a lower rate of ETE (14%) and LN metastases (29%) compared with MTCs with *RET* mutations (67% and 83%, respectively), these differences did not reach significance (p=0.10 for both variables).

Conclusions: 26% of MTCs in our cohort had an underlying *RAS* mutation. Tumors with *RAS* mutations appear to have a relatively low rate of ETE and LN metastases at presentation.

643 INSM1: A Novel Immunohistochemical Marker for Neuroendocrine and Neuroepithelial Neoplasms

JN Rosenbaum, R Baus, H Werner, CS Clifford, WM Rehrauer, RV Lloyd. University of Wisconsin Hospital & Clinics, Madison, WI.

Background: INSM1 is a transcription factor expressed during the normal development of neuroendocrine tissues and neuroepithelia. Molecular detection of INSM1 has been demonstrated throughout neural and neuroendocrine tissue in developing embryos. In adults, INSM1 has only been detected in neoplasms. The spatio-temporal restriction of INSM1 expression makes it an attractive candidate as a tumor marker, and confers advantages over traditional neuroendocrine markers.

Design: INSM1 is detected by immunohistochemistry (IHC) using a commercial antibody and established protocol. The antibody is validated on fetal autopsy tissue. Selecting specimens from the University of Wisconsin Department surgical pathology archives, we assay a spectrum of neuroendocrine and non-neuroendocrine neoplasms (**Table 1**). We grade the degree of staining from 0 - 3. Quantitative expression of INSM1 for a subset of samples is evaluated using qRT-PCR, and correlated IHC. INSM1 is directly compared against traditional neuroendocrine markers chromogranin and synaptophysin.

Results: Nuclear expression of INSM1 is detected in fetal neuroendocrine tissue. Among the adult tissues tested, INSM1 is detected in most neural and neuroendocrine neoplasms, and is not detected in non-neuroendocrine tumors or most healthy tissues (**Table 1**).

INSM1 is detected, though, in non-neoplastic pancreatic islets and Kulchitsky cells. Qualitiative analysis of IHC correlates closely with quantitative detection of INSM1 expression levels by qRT-PCR.

Table 1. Neoplasms Staining with INSM1

Tumor Type	Specimens Staining Positively / Total Specimens
Carcinoid (Lung)	6 / 6
Esthesioneuroblastoma	1 / 1
GI-NEN (GI carcinoid)	11 / 16
Hypothalamic Hamartoma	0 / 1
Large Cell NE Carcinoma	2 / 2
Medullary Thyroid Carcinoma	2 / 3
Medulloblastoma	2 / 2
Merkel Cell Carcinoma	6 / 6
Neuroendocrine Carcinoma of the Breast	1 / 1
Pan-NEN	7 / 8
Paraganglioma	9 / 9
Parathyroid Adenoma	0 / 4
Parathyroid Carcinoma	0 / 2
Pheochromocytoma	6 / 7
Pituitary Adenoma	4 / 6
Pituitary Carcinoma	3 / 3
Small Cell Carcinoma (Lung)	3 / 3
Adenocarcinoma	0 / 3
Anaplastic Thyroid Carcinoma	0 / 1
Follicular Thyroid Carcinoma	0 / 1
Melanoma	0 / 4
Total	89

Conclusions: As a nuclear protein, INSM1 staining is easier to interpret than cytoplasmic markers, and is independent of the number of cytoplasmic granules. Staining is both specific (100%) and sensitive (79%) to neural and neuroendocrine tumors, (though sensitivity does vary with tumor type - **Table 1**). INSM1 is a valuable tool in diagnosing neuroendocrine and neuroepithelial neoplasms.

644 Frequent Nuclear β-Catenin Expression in Adrenal Cortical Carcinoma: A Diagnostic Pitfall

MI Samuelson, EB Stelow, JL Hornick, AM Bellizzi. University of Iowa, Iowa City, IA; University of Virginia, Charlottesville, VA; Brigham and Women's Hospital, Boston, MA.

Background: β-catenin (BCAT) functions adjacent to the cell membrane (cell-cell adhesion) and in the nucleus (transcription of target genes). With *APC* inactivation or *CTNNB1* activation, predominant expression shifts from cell membrane to nucleus. "Aberrant" BCAT nuclear staining is increasingly relied on as a specific marker of certain tumors [e.g., desmoid fibromatosis, solid-pseudopapillary neoplasm (SPN)], despite incomplete categorization of BCAT expression in the wide range of tumors. We recently encountered a 45-year-old woman with a 10 cm solid/cystic mass, radiologically in the pancreatic tail. Cytology revealed a cellular, dyscohesive smear pattern. Based in part on nuclear BCAT expression, SPN was favored. At laparotomy, tumor was locally invasive and metastatic to peritoneum and liver; resection was aborted, but additional biopsies were taken. A broader differential was considered, with a diagnosis of adrenal cortical carcinoma (ACC) ultimately rendered. The purpose of this study is to examine BCAT expression in ACC, which, if frequently BCAT-nuclear-positive, would represent a significant pitfall in the diagnosis of SPN.

Design: BCAT immunohistochemistry was performed on 47 ACCs, as well as 10 adrenal cortical adenomas (ACAs) and 10 normal adrenals. The following were noted: 1. predominant pattern (membranous, nuclear or nuclear/cytoplasmic, perinuclear/dot-like, null); 2. extent (<10%; 10-50%; >50%, diffuse); 3. secondary staining pattern(s).

Results: Normal adrenals displayed a gradient of membranous expression—intense in zona (z.) glomerulosa, weaker in z. fasciculata, weakest in z. reticularis, absent in medulla. 66% of ACCs expressed BCAT, while 34% were null. Nuclear or nuclear/cytoplasmic staining was the predominant pattern in 21% and not seen as secondary patterns. Other predominant patterns were membranous (28%) and perinuclear/dot-like (17%). Expression was typically diffuse (77%), and mixed patterns (e.g., predominantly nuclear and focally membranous) were seen in a minority (23%). All 10 ACAs expressed BCAT, 9 predominantly membranous and 1 predominantly nuclear, with mixed patterns not unusual (60%).

Conclusions: Adrenal cortical neoplasms demonstrate various BCAT expression patterns, and nuclear expression is not uncommon, especially in ACCs, which represents a significant pitfall. In the broader sense, this study highlights the potential danger of overreliance on purportedly "specific" immunohistochemical markers whose full range of expression have yet to be elucidated.

645 Potential Pitfalls in SDH Immunohistochemistry to Detect Patients with Paraganglioma and Phaeochromocytoma Harbouring Germline *SDHx* Gene Mutations

R Santi, E Rapizzi, T Ercolino, G Baroni, L Canu, M Mannelli, G Nesi. University of Florence, Florence, Italy.

Background: Succinate dehydrogenase (SDH) is a complex encoded by 4 separate genes (*SDHA, SDHB, SDHC, SDHD*, collectively known as *SDHx*), any one of which can be mutated to cause hereditary phaeochromocytomas (PCC)/paragangliomas (PGL). Germline mutations in any of the *SDHx* genes result in destabilization of the SDH protein complex and loss of SDHB expression at immunohistochemistry (IHC). Consequently, IHC has been proposed to triage genetic testing, thus reducing time and costs. Recent complementary findings are that immunoreactivity for SDHA is lost together with SDHB in *SDHA*-mutated tumours, but is retained in tumours with other *SDH* mutations. We investigated whether SDHA/SDHB IHC could identify *SDHx*-related tumours in a retrospective case series.

Design: SDHA and SDHB IHC was performed in 13 *SDHx*-mutated tumours (*SDHB*: n=3; *SDHC*: n=1; *SDHD:* n=9) and 16 wild-type tumours. In all PCC/PGL, both enzymatic activity and protein expression were analyzed by Western Blot analysis. Immunohistochemically, definite granular cytoplasmic staining was scored as "positive", faint cytoplasmic blush was classified as "weak diffuse" staining and total lack of staining in the presence of an internal positive control as "negative".

Results: Enzymatic activity and protein expression were significantly reduced in tumours harbouring *SDHx* mutations compared with wild-type tumours. SDHB immunostaining detected 10/13 (76.9%) *SDHx*-mutated PCC/PGL (3/3 *SDHB*-mutated samples; 1/1 *SDHC*-mutated sample; 6/9 *SDHD*-mutated samples). In three *SDHD*-related tumours with the same mutation (p.Pro81Leu), positive (n=2) or weak diffuse (n=1) SDHB staining was observed. Wild-type PCC/PGL exhibited SDHB immunoreactivity (n=16/16). SDHA protein expression was preserved in all mutated tumours (n=13/13). In wild-type PCC/PGL, IHC for SDHA was positive in 15/16 (93.8%) cases and weak diffuse in one (1/16, 6.2%).

Conclusions: These findings suggest that SDHA and SDHB IHC should be considered with caution, due to possible false positive or false negative results. Furthermore, a weak diffuse pattern of staining may lead to misinterpretation of *SDH* gene status. In particular, *SDHD*-related tumours may remain undetected at immunohistochemical analysis.

646 MicroRNA Expression Profiling through Small RNA Sequencing Identified Molecular Subtypes of Pheochromocytoma and Paraganglioma

T Scognamiglio, Y-T Chen, Z Chen, T Tuschl, N Renwick. Weill Cornell Medical College, New York, NY; The Rockefeller University, New York, NY.

Background: MicroRNA expression profiles of pheochromocytomas (PCCs) and paragangliomas (PGLs) have been reported in 4 previous studies with variable results. These studies were based on microarray and/or PCR-based analyses and are limited by the pre-selected pool of miRNA species to be interrogated. In this study, we used small RNA sequencing to generate comprehensive miRNA expression profiles for PCCs and PGLs aiming at the identification of dysregulated miRNAs in these tumors.

Design: Total RNA was extracted from formalin-fixed paraffin-embedded tissue blocks of 10 PCCs (8 benign and 2 malignant) and 10 PGLs (9 benign and 1 malignant). Small RNA sequencing was performed using an input of 100ng of total RNA, yielding an average of 6.0 million miRNA sequence reads per sample. Unsupervised hierarchical clustering was performed using normalized miRNA counts, and lists of miRNA species that differentiated clusters were generated.

Results: PCCs/PGLs showed a distinctive miRNA profile and formed a distinctive cluster when analyzed with other neuroendocrine tumors (NETs) similarly profiled in our laboratory, including Merkel cell carcinoma, melanoma, and NETs from the pancreas and ileum. Moreover, unsupervised hierarchical clustering classified the 20 cases into two groups of 4 (Gr. I) and 16 cases (Gr. II), with Group I being characterized by the shutdown of a cluster of 16 miRNAs localized to chromosome 14q32. Group II could be further divided into two subgroups of 6 (Gr. IIa) and 10 cases (Gr. IIb). Group IIa consisted exclusively of PGLs, whereas group IIb was mostly PCCs (8 PCCs and 2 PGLs). These subgroups did not correlate with clinical behavior (benign vs. malignant) or other clinicopathological parameters. miRNA markers previously proposed to be potentially useful in distinguishing benign vs. malignant PCCs/PGLs, namely miR-483-5p, -101, and -183, were not found to be differentially expressed in our cohort.

Conclusions: Direct miRNA sequencing allowed comprehensive unbiased miRNA profiling of PCCs/PGLs and identified a panel of dysregulated miRNA. Our findings suggest two or three molecular subtypes of PCCs/PGLs that likely differ in their tumorigenesis. These differences are reflected in their miRNA profiles and the potential downstream targets of these dysregulated miRNAs are being explored.

647 Quantitation and Detection of *BRAF* V600E Mutation in Papillary Thyroid Carcinoma

D Sirohi, Y Wang, JR Lindner, K Vadlamudi, WB Furmaga, H Fan. University of Texas at Health Science Center at San Antonio, San Antonio, TX.

Background: The BRAF V600E mutation has been identified in thyroid cancer, mostly in papillary thyroid carcinoma (PTC) and anaplastic thyroid carcinoma (ATC). The mutation is a diagnostic marker, and may also be a prognostic marker. Mutation quantitation in PTCs is rarely reported. We evaluated the V600E frequency and mutation load in PTCs with a validated laboratory developed quantitative allelic discrimination real-time PCR (Q-AD-PCR) assay.

Design: Paraffin blocks were collected from 62 thyroid carcinomas between 01/2012 - 06/2013: 34 classic PTCs, 23 follicular variant PTCs (FV-PTC), and 5 others (2 ATC, 2 insular carcinoma, 1 follicular thyroid carcinoma). DNA was extracted from FFPE sections (estimated tumor load range 1-95% on the section) on all cases without macrodissection (MCD), and on 12 selected cases with MCD. Samples were analyzed for the mutation and mutation load by Q-AD-PCR assay. The relative quantitation of V600E is determined by comparing results to a V600E homozygous melanoma cell line (ATCC HTB-72D). The correlation between the mutation load and clinical parameters were statistically evaluated using the Student's t-test.

Results: V600E was detected in 38.2% classic PTCs and 17.4% FV-PTCs. No significant correlation was found between mutation load and patient's age, sex, or tumor type (P >0.1). However, patient's tumor size was associated with mutation load (P=0.0008). The detected mutation load is also positively correlated to the tumor load on FFPE section (correlation coefficient of 0.7).

Characteristic		Mutation frequency (%)	Mutation load median% (range)
Age	≤45	5/25 (20%)	33 (9-65)
	>45	12/37 (32.4%)	31 (8-59)
Sex	Male	5/13 (38.4%)	48 (8-65)
	Female	12/49 (24.5%)	31 (9-54)
Subtype	PTCs	13/34 (38.2%)	28 (8-65)
	FV-PTCs	4/23 (17.4%)	36 (33-54)
	Others	0/5 (0%)	0
Tumor size	<4 cm	15/55 (27.2%)	33 (8-54)
	>4 cm	2/7 (28.5%)	62 (59-65)

The MCD step detected 2 more V600E positive classic PTCs with lower tumor load (<25%), increasing the mutation frequency in classic PTCs to 44% (15/34). MCD also increased the detected mutation load from 0-33% to 40-64% on 7 cases with tumor load ≤30%.

Conclusions: V600E was detected in classic PTCs and FV-PTCs with the median mutation load below 50%, suggesting most PTC tumor cells carry heterozygous mutations. The positive correlation between mutation load and tumor load on the section indicates that the mutation was present in tumor cells. A MCD step is helpful to enrich tumor cells on FFPE sections with low tumor load. In our limited PTC cases, only tumor size was correlated to the V600E mutation load.

648 Cadherin 17 Is a Sensitive Marker of Midgut and Hindgut Neuroendocrine Tumors

AN Snow, S Mangray, R Clubwala, J Li, R Monahan, M Resnick, E Yakirevich. Alpert Medical School of Brown University, Providence, RI.

Background: Cadherin 17 (CDH17) is a member of the superfamily of calcium dependent cell adhesion molecules. Expression of CDH17 has been shown to be limited to normal intestinal epithelium and digestive tract tumors and has not been detected in tumors from other sites. We investigated whether CDH17 is differentially expressed in digestive system neuroendocrine tumors (NETs) as opposed to pulmonary NETs and compared its expression with CDX2 and TTF-1 as markers of intestinal and pulmonary differentiation.

Design: One hundred fifty cases of low-to intermediate grade NETs including 68 foregut (39 lung carcinoids, 10 gastric and 14 pancreatic), 70 midgut (36 small intestinal (SI) and 15 appendiceal) and 12 hindgut (distal colon and rectal) were studied. Tissue microarrays were analyzed for IHC expression of CDH17, CDX2 and TTF-1. Immunoreactivity was assessed based on a combined score of extent and intensity.

Results: Normal intestinal and pancreatic ductal epithelium expressed strong membranous CDH17 staining with lateral intercellular border accentuation. In NETs the CDH17 staining pattern was membranous independent of location. CDH17 immunoreactivity increased significantly from foregut NETs through hindgut tumors (P<0.0001). Within the foregut, pancreatic NETs expressed CDH17 at significantly higher frequency (42.9%) as opposed to other foregut tumors (P<0.012). The vast majority of midgut NETs were positive for CDH17 (92.9%) and CDX2 (84.5%). Both appendiceal and SI NETs were more frequently positive for CDH17 as compared to CDX2 (100% and 92.5% vs 86.7% and 86.8%). The combination of CDH17 and CDX2 did not increase the sensitivity for the identification of midgut NETs when compared with CDH17 alone. All hindgut NETs expressed CDH17 in contrast to only one rectal NET (8.3%) which was positive for CDX2. The majority (76.9%) of lung carcinoids were positive for TTF-1, while all midgut and hindgut carcinoids were negative (P<0.0001).

	Number (%) positive		
NET Site	**CDH17**	**CDX2**	**TTF-1**
Lung (N=39)	3(7.7)	0(0)	30(76.9)*
Stomach (N=10)	2(20)	1(10)	0(0)
Duodenum (N=5)	1(20)	3(60)	0(0)
Pancreas (N=14)	6(42.9)*	2(14.3)	0(0)
Foregut Combined (N=68)	12(17.6)	6(8.8)	30(44.1)*
Small Bowel Distal to Ampulla (N=55)	49(92.5)	46(86.8)	0(0)
Appendix (N-15)	15(100)	13(86.7)	0(0)
Midgut Combined (N=70)	65(92.9)*	60(84.5)*	0(0)
Hindgut (Rectum and distal Colon, N=12)	12(100)*	1(8.3)	0(0)

*P values range from .012 to <0.0001

Conclusions: This study is the first to comprehensively examine CDH17 expression in NETs from different sites. CDH17 is a highly sensitive marker for midgut NETs and in contrast to CDX2 is a reliable marker of hindgut NETs.

649 Extensive Evaluation of Immunohistochemistry to Assign Site of Origin in Well-Differentiated Neuroendocrine Tumors: A Study of 10 Markers in 265 Tumors

KM Stashek, TW Czeczok, AM Bellizzi. University of Iowa, Iowa City, IA; University of Pennsylvania, Philadelphia, PA.

Background: Determining the site of origin of a well-differentiated neuroendocrine tumor (NET) is prognostically and, increasingly, therapeutically significant. Immunohistochemistry (IHC) for TTF-1 (lung), CDX2 (midgut), polyclonal PAX8 (pPAX8; pancreatoduodenum/rectum), and islet 1 (ISL1; pancreatoduodenum/rectum) has been well-vetted in this setting. Several other markers have shown promise, but have been studied in smaller numbers of tumors and/or at a limited set of anatomic sites.

Design: IHC for TTF-1 (clones 8G7G3/1 and SPT24), CDX2, pPAX8, ISL1, PDX1, prostatic acid phosphatase (PrAP), NESP55, PR, and PAX6 was performed on tissue microarrays (TMAs) and whole sections of the following NETs: 20 lung, 14 stomach, 22 duodenum, 70 pancreas (57 primary, 13 metastatic), 107 jejunoileum (66 primary, 41 metastatic), 15 appendix, 17 rectum. For this abstract, any definite staining was considered positive.

Results: Frequency of expression of 4 well-vetted and 6 extended markers are presented in Tables 1 and 2. For PrAP-positive jejunoileal tumors, staining often predominated at the periphery of nests.

Table 1: Expression of Well-Vetted Markers*

	TTF-1 (clone 8G7G3/1)	CDX2	pPAX8	ISL1
Lung	35	5	0	0
Stomach	0	7	0	7
Duodenum	0	48	5	82
Pancreas primary	0	14	2	91
Pancreas metastatic	0	0	0	85
Jejunoileum primary	0	97	0	2
Jejunoileum metastatic	0	83	0	2
Appendix	0	100	0	47
Rectum	0	12	0	87

* Data are % positive

Table 2: Extended Marker Evaluation*

	TTF-1 (clone SPT24)	PDX1	PrAP	NESP55	PR	PAX6
Lung	50	10	0	65	5	0
Stomach	0	43	0	14	7	0
Duodenum	0	100	0	71	14	62
Pancreas primary	0	88	5	75	67	79
Pancreas metastatic	0	85	8	54	69	69
Jejunoileum primary	0	32	59	24	3	0
Jejunoileum metastatic	0	10	37	15	7	0
Appendix	0	71	43	86	14	20
Rectum	0	94	88	35	19	56

* Data are % positive

Conclusions: TTF-1 is specific for lung; the newer SPT24 clone appears more sensitive. CDX2 is very sensitive and fairly specific for jejunoileum. ISL1 and PDX1 are sensitive for pancreatoduodenum, though rectal and appendiceal tumors are also often positive. Results with pPAX8 were disappointing, possibly reflecting lot-to-lot variation for this polyclonal antibody; data for PAX6 were similar to those published for pPAX8. In addition to rectal tumors, PrAP stained a significant number of jejunoileal tumors in a characteristic pattern. NESP55 was widely expressed. PR was reasonably sensitive and specific for pancreas, with retained expression in metastases. Of the extended markers, we are likely to incorporate TTF-1 SPT24, PAX6, PrAP, and PR into our practice.

650 Papillary Thyroid Carcinoma in Patients with Hashimoto's Thyroiditis – A Clinicopathologic Study of 59 Cases

D Suster, P Ortega-Espinosa, S Suster. Medical College of Wisconsin, Milwaukee, WI.

Background: Although the association between papillary thyroid carcinoma (PTC) and Hashimoto's thyroiditis (HT) has been known for more than 50 years, the clinicopathological features of this association have not been well characterized.

Design: We reviewed 209 cases of HT accessioned over a 15-year period (1994-2008) and identified 59 patients who had coexisting PTC with HT.

Results: The patients ranged in age from 15 to 81 years (median: 44); 55 were women and 4 were men. The tumors measured from 0.1 to 5.30 cm in diameter (median: 1.55cm). Most of the tumors were unifocal, well circumscribed and confined to the thyroid gland. Histologically, 22 were oncocytic (37.3%), 20 were conventional type (33.9%), 13 were follicular variant (22%), 2 were tall cell (3.4%), 1 was solid and cribriform (1.7%) and 1 was columnar cell type (1.7%). All of the cases in our study showed the classical optically clear nuclei of PTC, nuclear grooves and intranuclear cytoplasmic inclusions. Extrathyroidal extension was present in five cases, most of them corresponding to high-grade histology tumors (tall cell, solid and columnar variant). Three of the cases of PTC with high-grade histology showed vascular invasion. Cervical lymph node metastases were documented in 20 cases (32.8%) at the time of diagnosis. Clinical follow up from 11 to 186 months (median: 64.5 mos) in 51 patients showed that all of them were alive and well and free of disease at last follow-up. Recurrences to cervical lymph nodes were noted after 53, 40, 24 and 11 months (median: 32) in four patients. No tumor-related deaths were observed in this cohort.

Conclusions: Our findings suggest no differences in behavior between papillary carcinoma histologic subtypes in patients with HT, except for high grade variants of papillary carcinoma, most of which presented with extrathyroidal extension and vascular invasion at initial diagnosis. Overall, the incidence of papillary carcinoma in our patients with Hashimoto's thyroiditis was 28.2%. With the exception of the high-grade histology cases, the favorable outcome observed in this study for the more conventional histologic variants of PTC, with low recurrence rates and no mortality, suggests a probable immunologic mechanism that may limit tumor growth and metastasis in patients with Hashimoto's thyroiditis.

651 Papillary Thyroid Carcinoma and Chronic Lymphocytic Thyroiditis, Linked by Severity of Chronic Inflammation or Anti-Thyroid Autoantibodies?

JNM Tan, A de las Morenas. Boston University Medical Center, Boston, MA.

Background: The relationship between chronic inflammation and tumorigenesis is well-established in many types of neoplasms. Many authors have studied this relationship in thyroid cancers especially the association of chronic lymphocytic thyroiditis (CLT) with papillary thyroid carcinoma (PTC). Data show higher prevalence of PTC in patients with chronic inflammation. Many mechanisms have been proposed such as stimulation of the thyroid by inflammatory cells and molecular studies linking specific mutations in PTC to CLT. Despite the accumulation of data, there remains a controversy regarding this topic. The question of whether chronic lymphocytic infiltrate (CLI) plays a role in carcinogenesis or is a component of autoimmunity remains unanswered. In this study, we aim to determine the possible association of PTC with chronic thyroiditis according to the severity of CLI and presence anti-thyroid autoantibodies (ATA).

Design: We performed a retrospective review of the pathology of 749 patients who underwent thyroidectomy at our institution from 1/2010 to 7/2013. 297 cases with chronic thyroiditis were identified and 196 had either an anti-thyroglobulin or anti-thyroid peroxidase antibody testing done. 4 cases with malignancies other than PTC were excluded. 192 cases were included, 102 had positive ATA. We compared the final histologic diagnoses according to the presence of ATA and the severity of CLI.

Results: Our study demonstrated a higher rate of PTC in cases with CLT compared to benign thyroid disease (62% vs 38%, p<.0001). After comparing the cases according to the severity of CLI and presence of ATA, the results were not statistically significant.

Table 1. Final diagnoses of cases with CLT, number (%)

	With CLT	Without CLT	P
PTC	119 (62%)	170 (31%)	<0.0001
Benign thyroid	73 (38%)	387 (69%)	

CLT=chronic lymphocytic thyroiditis

Table 2. Final diagnoses of cases with CLT according to the presence of ATA and severity of chronic inflammation, number (%)

	Benign thyroid	PTC	P
With ATA	38 (37%)	64 (63%)	0.8819
Without ATA	35 (39%)	55 (61%)	
Mild CLI	44 (39%)	69 (61%)	0.7651
Moderate to severe CLI	29 (37%)	50 (63%)	

ATA=antithyroid autoantibody, CLI=chronic lymphocytic infiltrate

Conclusions: Chronic thyroiditis is associated with significantly higher risk of PTC, likely due to inflammatory microenvironment. The severity of CLI and the presence of ATA such as anti-thyroglobulin or anti-thyroid peroxidase antibody which are considered hallmarks of autoimmunity do not appear to be specifically associated with this risk.

652 BRAF V600E Mutation in Anaplastic Thyroid Carcinoma

AE Walts, A Pao, S Bose. Cedars-Sinai Medical Center, Los Angeles, CA.

Background: Anaplastic thyroid carcinoma (ATC) is an uncommon but highly aggressive tumor that is characteristically refractory to radioiodine therapy. BRAF mutation has been reported in up to 40% of ATC. Identification of a differentiated or poorly differentiated cancer component in some ATC raises the possibility of transition from a differentiated carcinoma. Recently, targeted therapy with Vemurafenib has shown some efficacy in BRAF mutated ATC. Intratumoral heterogeneity is recognized as an important determinant of a cancer's response to targeted therapy. This study was designed to assess BRAF genetic heterogeneity (BRAF GH) within ATC.

Design: 13 ATC [9 with area(s) of differentiated or poorly differentiated papillary thyroid carcinoma (ATC-PTC) and 4 without differentiated area(s) (ATC-ATC)] were identified in our database. After slides were reviewed, diagnoses confirmed, and patient demographics recorded, formalin fixed paraffin embedded sections of the ATCs were macrodissected and analyzed for BRAF V600E (1799T>A) mutation using real-time PCR. BRAF GH was assessed in 2 groups of paired tumor samples: ATC-PTC group: PTC component vs. anaplastic component in the same tumor ATC-ATC group: two separate areas of anaplastic tumor in ATC without PTC component.

Results: The 13 patients (8 females, 5 males) ranged from 70 to 89 years in age (median 76 yrs) at operation. The tumors ranged from 3.5 cm to 9.0 cm. The BRAF mutation was detected in 9 (69.2%) of the cases including 7 (77.8%) of the ATC-PTC and in 2 (50%) of the ATC-ATC tumors. Analysis for the presence of the BRAF mutation yielded concordant results in 100% of the paired samples.

Conclusions: BRAF V600E mutation occurs frequently in ATC and its incidence is higher in ATC that exhibit a PTC component than in those that lack this feature. Heterogeneity for BRAF mutation status is infrequent within primary ATCs. Our findings support PTC as the origin of a subset of ATC and suggest that the BRAF mutation is an early event in their development. Testing for the presence of BRAF V600E mutation may improve therapy selection in ATC.

653 Phosphohistone H3 (PHH3) Is a Reliable Proliferation Marker in Grading Pulmonary and Pancreatogastrointestinal Neuronendocrine Neoplasms

W Zhou, J Balakrishna, V Ghali. St. Luke's - Roosevelt Hospital, New York, NY.

Background: Pathologic grading of neuroendocrine tumors (NET) is established by scoring the number of mitoses per 10 high-power fields (/10 HPF), and immunostaining of proliferating cell nuclear antigen or MIB-1/Ki-67. However, Ki-67 is expressed throughout the cell cycle from late G1 phase. Many Ki-67+ nuclei may not survive the cell cycle and are driven into apoptosis, thereby blurring the prognostic value. Anti-PHH3 antibody detects specifically the core protein histone H3 only when phosphorylated at serine 10 or serine 28 - a process almost exclusively occurring during mitosis.

Design: We studied anti-PHH3 staining in 41 cases of pulmonary and 39 cases of pancreatogastrointestinal NET. We compared anti-PHH3/10 HPF with MIB/Ki-67 and H&E mitosis/10 HPF. The staining of PHH3 was evaluated by counting of positive nuclei (×400). In general, the staining of PHH3 was strong and crisp even at cauterized areas, with no background. Some interphase nuclei with sparse granular staining were not counted. 80 cases were scored blindly by two observers showing good agreement (Spearman's correlation coefficient 0.81, $\kappa = 0.70$).

Results: The median of PHH3-positive mitotic figures were 1.1, 8.5 and 52/10HPF for grade 1, grade 2 (atypical) and grade 3 (small cell carcinoma) of pulmonary NET. The median of PHH3-positive mitotic figures for pancreatogastrointestinal NET were 0.8, 5.5 and 22 for grade 1, grade 2 and grade 3 NET (Table 1). Increasing PHH3-positive mitotic figures was strongly correlated to increased tumor grading ($P<0.001$; Mann–Whitney). The PHH3 positive figures, H&E mitotic count and Ki67 index were well correlated (Spearman's correlation coefficient 0.62, $P<0.001$). Only 6 cases (67%) of grade 3 pulmonary NET and 3 cases (43%) grade 3 GI NET showed some PHH3 negative mitotic figures (<10% of total mitotic cells). In 10 pulmonary grade 2 NET, 4 cases with distance metastasis (bone, liver) had higher PHH3 count (>10/10HPF, average 12/10HPF), raising the possibility that these tumors should be upgraded.

Conclusions: PHH3 is a rapid and reliable method assessing mitotic figures in grading pulmonary and GI neuronendocrine neoplasms.

Table 1. Mitotic count, Ki67 and PHH3 count in association with tumor grading

		PHH3/10HPF		Mitotic count /10HPF		Ki-67	
	N	Median	P-value	Median	P-value	Median	P-value
Lung			0.001<		0.001<		0.001<
G1	20	1.1		0.8		1.5	
G2	10	8.5		6.2		14	
G3	9·	52		60		88	
GI			0.001<		0.001<		0.001<
G1	28	0.8		0.6		1.5	
G2	4	5.5		3.5		22.5	
G3	7	22		23.5		48	

* 2 cases were excluded due to limited tissue amount (< 3HPF)·

Gastrointestinal Pathology

654 Endoscopic Abnormalities of the Pre-Pouch Ileum Are Strongly Predictive of Subsequent Crohn's Disease in Patients with an Ileal Pouch-Anal Anastomosis

CA Adackapara, A Agoston, M Hamilton, RD Odze, A Srivastava. Brigham and Women's Hospital, Boston, MA.

Background: Approximately 10% of patients with an ileal pouch-anal anastomosis (IPAA) for ulcerative colitis (UC) develop refractory pouchitis or have their diagnoses revised to Crohn's disease (CD) on follow up. The clinical and pathologic features best predictive of pouch revision/failure and a revised diagnosis of CD are unknown. The aim of our study was to determine the significance of pre-pouch abnormalities as a predictor of pouch revision/failure and CD.

Design: 152 patients with IPAA for UC, identified over a 20 year period at a tertiary academic medical center, were evaluated. For each patient, the presence and type of endoscopic abnormalities in the pre-pouch ileum, a histologic diagnosis of pre-pouch ileitis, the number of episodes of clinical pouchitis, and the presence of refractory pouchitis were recorded. The major outcomes of interest were pouch revision/failure and a revised diagnosis of CD. Multivariate linear regression analysis was performed to identify features most predictive for the outcomes above.

Results: 71 men and 81 women (mean age 51.7 years) with a mean follow-up of 12.2 years (range 1-31 years) formed the study group. 40/152 patients had pre-pouch ileitis on biopsy whereas 27/152 had endoscopic abnormalities noted in the pre-pouch ileum (including erythema, erosion, ulcer, and stricture). The mean number of episodes of clinical pouchitis for all patients was 2.2. Sixteen (10%) patients developed refractory pouchitis, 20 patients (13%) had pouch revision/failure and 18 (12%) had a diagnosis revised to CD on follow-up. The presence of any pre-pouch abnormality on endoscopy (OR 3.86; p=0.034), refractory pouchitis (OR 5.17; p=0.015), and a revised diagnosis of CD (OR 4.30; p=0.025) were predictive of pouch revision/failure unrelated to surgical issues. In addition, more than 2 episodes of clinical pouchitis (OR 7.54; p=0.002), pre-pouch abnormality on endoscopy (OR 6.91; p=0.002), and pre-pouch ileitis either by endoscopy or biopsy (OR 3.28; P=0.049) were most predictive of a subsequent diagnosis of CD.

Conclusions: Refractory pouchitis and endoscopic abnormalities of the pre-pouch ileum are most predictive of eventual pouch revision/failure. Multiple episodes of clinical pouchitis and pre-pouch abnormalities on endoscopy are strong predictors of a revised diagnosis of CD.

655 The Expression of CD44v6 in Colon: From Normal to Malignant

A Afify, A Virdi, H Jess. UC Davis, Sacramento, CA.

Background: CD44v6, an integral transmembrane protein belonging to a family of adhesion molecule receptors, plays an important role in tumor growth, proliferation, and metastasis. Its expression in normal tissue is highly restricted. Transfection of tumor cells with CD44v6 exons confers an aggressive metastatic behavior. The purpose of this study was to evaluate the expression of CD44v6 in benign, hyperplastic, dysplastic and malignant colonic epithelium.

Design: Formalin-fixed, paraffin-embedded archival tissue from 178 cases of normal colonic tissue (n=25), hyperplastic polyps (HP, n=45), tubular adenomas (TA, n=57), villous adenomas (VA, n=25) and adenocarcinomas (n=26) of the colon were retrieved from the surgical pathology files. All cases were reviewed histologically for diagnosis confirmation and stained using a monoclonal antibody to CD44v6 (1:1500, Bender MedSystems). Positive staining was defined as uniform strong membranous staining in at least 10% of cells. The staining intensity (0+ to 3+) and distribution (focal vs diffuse) was assessed in a semi-quantitative fashion and scored.

Results: All cases of normal colonic tissue and HP expressed strong (3+) CD44v6 staining limited only to the cells located at base of the crypt. CD44v6 was expressed in 49 (86%) cases of TA (3+ in 30 cases and 2+ in 19 cases) and 18 (72%) cases of VA (3+ in 8 cases and 2+ in 10 cases). In both TA and VA the epithelial cells at the base of the crypt were negative, while the surface adenomatous epithelium showed diffuse CD44v6 staining. CD44v6 was expressed diffusely in 24 (92%) of adenocarcinomas (3+ in 13 cases, 2+ in 11 cases). Stromal cells in normal, benign or neoplastic lesions did not express CD44v6.

Conclusions: In normal colonic epithelium CD44v6 is exclusively expressed in cells located at the base of the crypt, the same location of colonic epithelial stem and progenitor cells. The gain of expression of CD44v6 in surface epithelium with loss of